

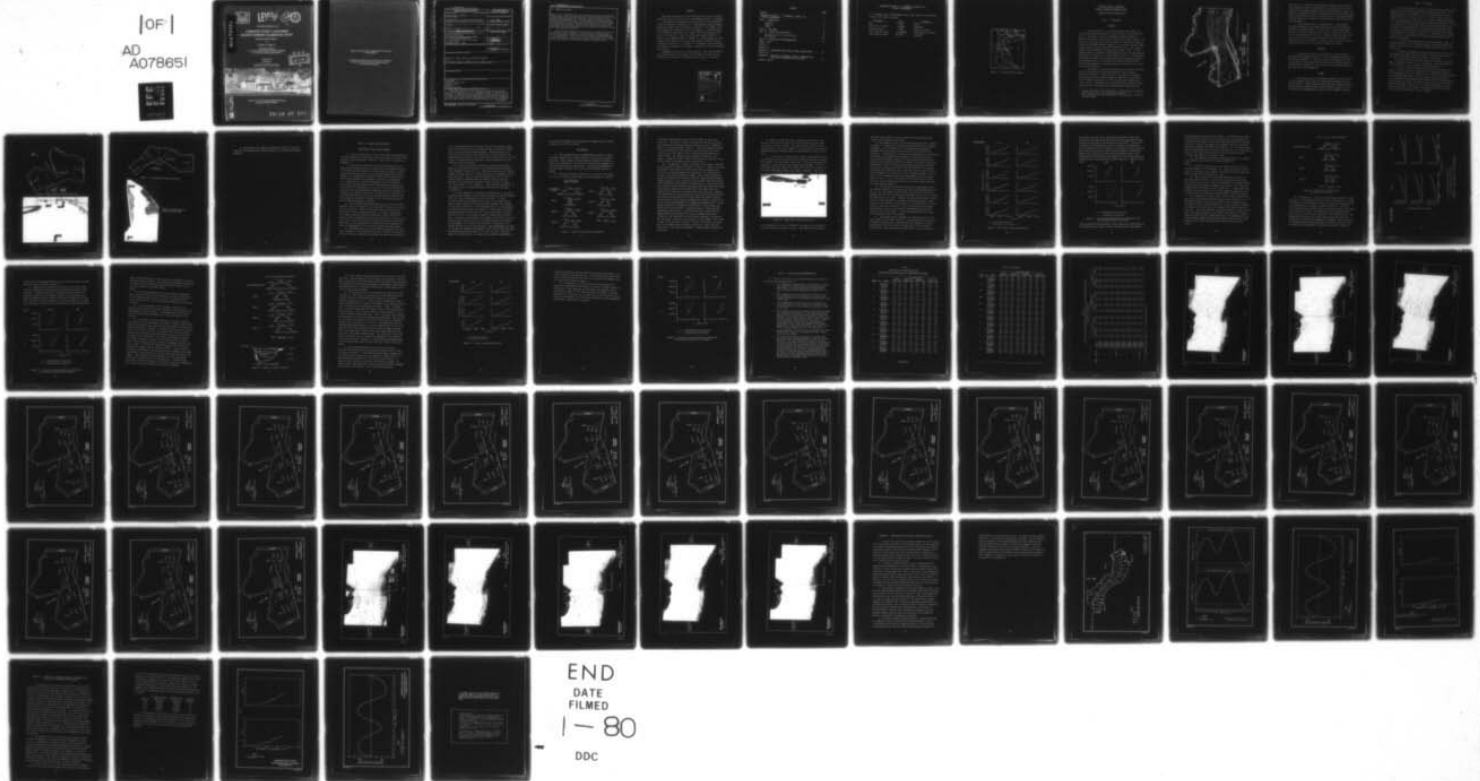
AD-A078 651

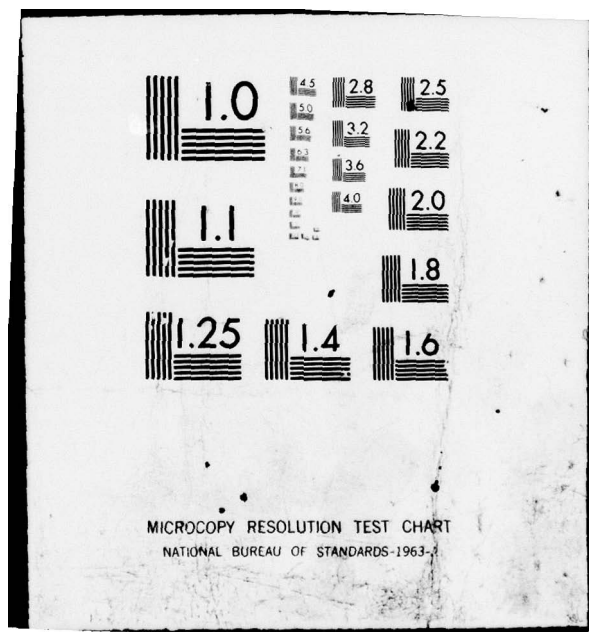
ARMY ENGINEER WATERWAYS EXPERIMENT STATION VICKSBURG--ETC F/G 8/8
CARQUINEZ STRAIT, CALIFORNIA, SALINITY BARRIER CALIBRATION STUD--ETC(U)
NOV 79 R C BERGER, M J TRAWLE
WES/HL-TR-79-18

UNCLASSIFIED

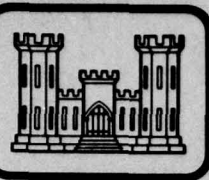
NL

|OF|
AD
A078651





ADA 078651



LEVEL



TECHNICAL REPORT HL-79-18

CARQUINEZ STRAIT, CALIFORNIA SALINITY BARRIER CALIBRATION STUDY

Hydraulic Model Investigation

by

Rutherford C. Berger, Jr.

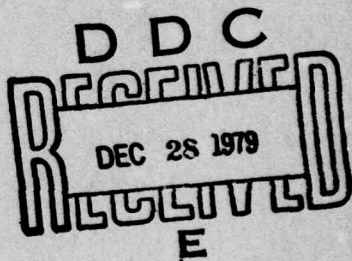
Hydraulics Laboratory

U. S. Army Engineer Waterways Experiment Station
P. O. Box 631, Vicksburg, Miss. 39180

November 1979

Final Report

Approved For Public Release; Distribution Unlimited



DDC FILE COPY

Prepared for U. S. Army Engineer District, Sacramento
Sacramento, California 95814

79-12 27 288

Destroy this report when no longer needed. Do not return
it to the originator.

The findings in this report are not to be construed as an official
Department of the Army position unless so designated
by other authorized documents.

Unclassified

SECURITY CLASSIFICATION OF THIS PAGE (When Data Entered)

REPORT DOCUMENTATION PAGE		READ INSTRUCTIONS BEFORE COMPLETING FORM
1. REPORT NUMBER Technical Report HL-79-18	2. GOVT ACCESSION NO.	3. RECIPIENT'S CATALOG NUMBER
4. TITLE (and Subtitle) CARQUINEZ STRAIT, CALIFORNIA, SALINITY BARRIER CALIBRATION STUDY; Hydraulic Model Investigation	5. TYPE OF REPORT & PERIOD COVERED Final report.	
6. 7. AUTHOR(s) Rutherford C. Berger, Jr. M. J. Trawles	8. CONTRACT OR GRANT NUMBER(s) 14 WES / HL-TR-79-18	
9. PERFORMING ORGANIZATION NAME AND ADDRESS U.S. Army Engineer Waterways Experiment Station Hydraulics Laboratory P. O. Box 631, Vicksburg, Miss. 39180	10. PROGRAM ELEMENT, PROJECT, TASK AREA & WORK UNIT NUMBERS 12 72	
11. CONTROLLING OFFICE NAME AND ADDRESS U. S. Army Engineer District, Sacramento 650 Capitol Mall Sacramento, Calif. 95814	12. REPORT DATE Nov 1979	
13. NUMBER OF PAGES 62	14. MONITORING AGENCY NAME & ADDRESS (if different from Controlling Office)	
15. SECURITY CLASS. (of this report) Unclassified		
15a. DECLASSIFICATION/DOWNGRADING SCHEDULE		
16. DISTRIBUTION STATEMENT (of this Report) Approved for public release; distribution unlimited. 9 Final rep't. Apr 77 - Apr 78		
17. DISTRIBUTION STATEMENT (of the abstract entered in Block 20, if different from Report)		
18. SUPPLEMENTARY NOTES		
19. KEY WORDS (Continue on reverse side if necessary and identify by block number) Calibrating Carquinez Strait, Calif. Hydraulic models Salinity Salt water barriers Also		
20. ABSTRACT (Continue on reverse side if necessary and identify by block number) The primary objective of this study was to develop three distorted-scale salinity barriers for use in a comprehensive model of the San Francisco Bay-Delta. In addition, tests were conducted to define the influence of the structures on velocities and flow distribution as they may affect navigation or cause erosion and as the model distortion may affect velocity distribution. The tests were conducted in a 1:100 undistorted-scale model that reproduced (Continued)		

DD FORM 1 JAN 73 1473 EDITION OF 1 NOV 65 IS OBSOLETE

Unclassified
SECURITY CLASSIFICATION OF THIS PAGE (When Data Entered)

411 389

Unclassified

SECURITY CLASSIFICATION OF THIS PAGE(When Data Entered)

20. ABSTRACT (Continued)

about 2 miles of Carquinez Strait and a 1:100 vertical and 1:1000 horizontal distorted-scale model that reproduced about 4 miles of Carquinez Strait. The distorted-scale model included an artificial bend that exists in the San Francisco Bay-Delta model. All tests were conducted with steady-state flow in both ebb and flood directions. The head losses for each salinity barrier were defined for a range of discharges in both ebb and flood directions in the undistorted-scale model. Tests were then conducted in the distorted-scale model with various crest widths and side slopes of the salinity barriers until head losses were duplicated.

Velocities were measured at 23 locations in the undistorted-scale model at 500,000 cfs with and without the salinity barrier to define changes in velocity distribution. Velocities were also measured at selected stations in the distorted-scale structure to define the influence of model distortion or flow distribution. Surface current patterns were defined for the salinity barrier that resulted in the highest probability of adverse erosion.

Unclassified

SECURITY CLASSIFICATION OF THIS PAGE(When Data Entered)

PREFACE

The model investigation reported herein was the result of studies authorized 29 March 1977 by the U. S. Army Engineer District, Sacramento.

The study was performed during the period April 1977 through April 1978 by the Hydraulics Laboratory, U. S. Army Engineer Waterways Experiment Station (WES), under the direction of Messrs. H. B. Simmons, Chief of the Hydraulics Laboratory, and F. A. Herrmann, Jr., Assistant Chief of the Hydraulics Laboratory; R. A. Sager, Chief of the Estuaries Division; R. A. Boland, Jr., Chief of the Interior Channel Branch; M. J. Trawle, Project Manager; and R. C. Berger, Jr., Project Engineer. Technicians of the Estuaries Division who were directly involved in the investigation were Messrs. J. S. Ashley, A. J. Banchetti, and D. Marzette. This report was prepared by Mr. Berger. Appendices A and B were prepared by Mr. Trawle.

Commanders and Directors of WES during the study and the preparation and publication of this report were COL John L. Cannon, CE, and COL Nelson P. Conover, CE. Technical Director was Mr. F. R. Brown.

Accession For	
NTIS GRA&I	<input checked="" type="checkbox"/>
DDC TAB	<input type="checkbox"/>
Unannounced	<input type="checkbox"/>
Justification _____	
By _____	
Distribution/ _____	
Availability Codes _____	
Dist	Avail and/or special
A	

CONTENTS

	<u>Page</u>
PREFACE	1
CONVERSION FACTORS, U. S. CUSTOMARY TO METRIC (SI)	
UNITS OF MEASUREMENT	3
PART I: INTRODUCTION	5
Problems	5
Objective	7
Scope	7
PART II: THE MODEL	8
PART III: MODEL TESTS AND RESULTS	12
Description of Tests and Procedures	12
Test Results	14
PART IV: CONCLUSIONS AND RECOMMENDATIONS	30
TABLES 1 AND 2	
PHOTOS 1-8	
PLATES 1-18	
APPENDIX A: UNDISTORTED-SCALE PHYSICAL MODEL VERIFICATION	A1
PLATES A1-A4	
APPENDIX B: REDUCTION IN DISCHARGE CAUSED BY SUBMERGED SILL: STEADY-STATE COMPARED WITH TIDAL MODE	B1
PLATES B1 AND B2	

CONVERSION FACTORS, U. S. CUSTOMARY TO METRIC (SI)
UNITS OF MEASUREMENT

U. S. customary units of measurement used in this report can be converted to metric (SI) units as follows:

Multiply	By	To Obtain
feet	0.3048	metres
miles (U. S. statute)	1.609344	kilometres
feet per second	0.3048	metres per second
cubic feet per second	0.02831685	cubic metres per second
tons (2,000 lb, mass)	907.1847	kilograms

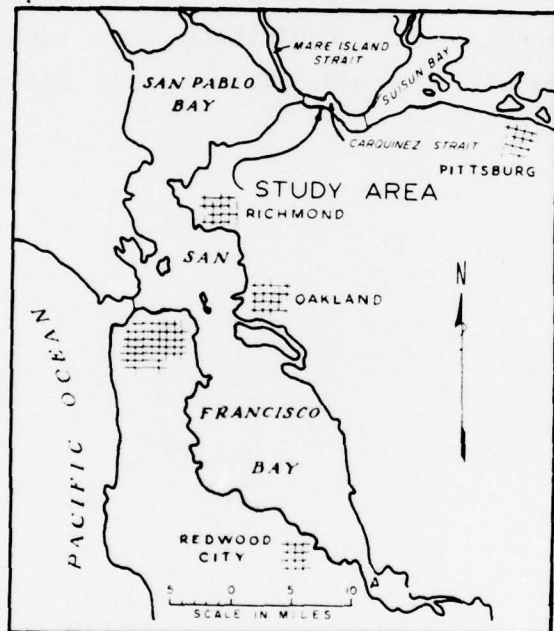


Figure 1. San Francisco Bay system

CARQUINEZ STRAIT, CALIFORNIA
SALINITY BARRIER CALIBRATION STUDY
Hydraulic Model Investigation

PART I: INTRODUCTION

Problems

1. Carquinez Strait is a relatively narrow, deep channel connecting Suisun and San Pablo Bays in the San Francisco Bay system (Figure 1). This strait is part of a deepwater navigation channel to Stockton, California, from the Pacific Ocean. The natural depths in the strait are quite deep (over 120 ft* at mllw** in some places, Figure 2); therefore no man-made channels through it are necessary. However, many of the shallower bay and river areas along the course of the navigation channel require dredging to achieve project depths. The U. S. Army Engineer District, Sacramento, investigated the effects of deepening the ship channel to Stockton to a project depth of -35 ft. In the course of conducting the study, it was anticipated that this deepening would have the detrimental effect of increasing the salinity intrusion inland. Barriers were proposed for Carquinez Strait as a possible way to reduce the salinity intrusion.

2. The impact of these salinity barriers was found by conducting tests in the San Francisco Bay-Delta hydraulic model located in Sausalito, California. Tides, salinities, and velocities throughout the San Francisco Bay estuarine system are reproduced in the model at a scale (model to prototype) of 1:100 vertically and 1:1000 horizontally. Prior to conducting tests in the San Francisco Bay-Delta model, structures had to be developed that reproduced the proper hydraulic

* A table of factors for converting U. S. customary units of measurement to metric (SI) units is presented on page 3.

** All elevations (el) cited herein are in feet referred to mean lower low water (mllw).

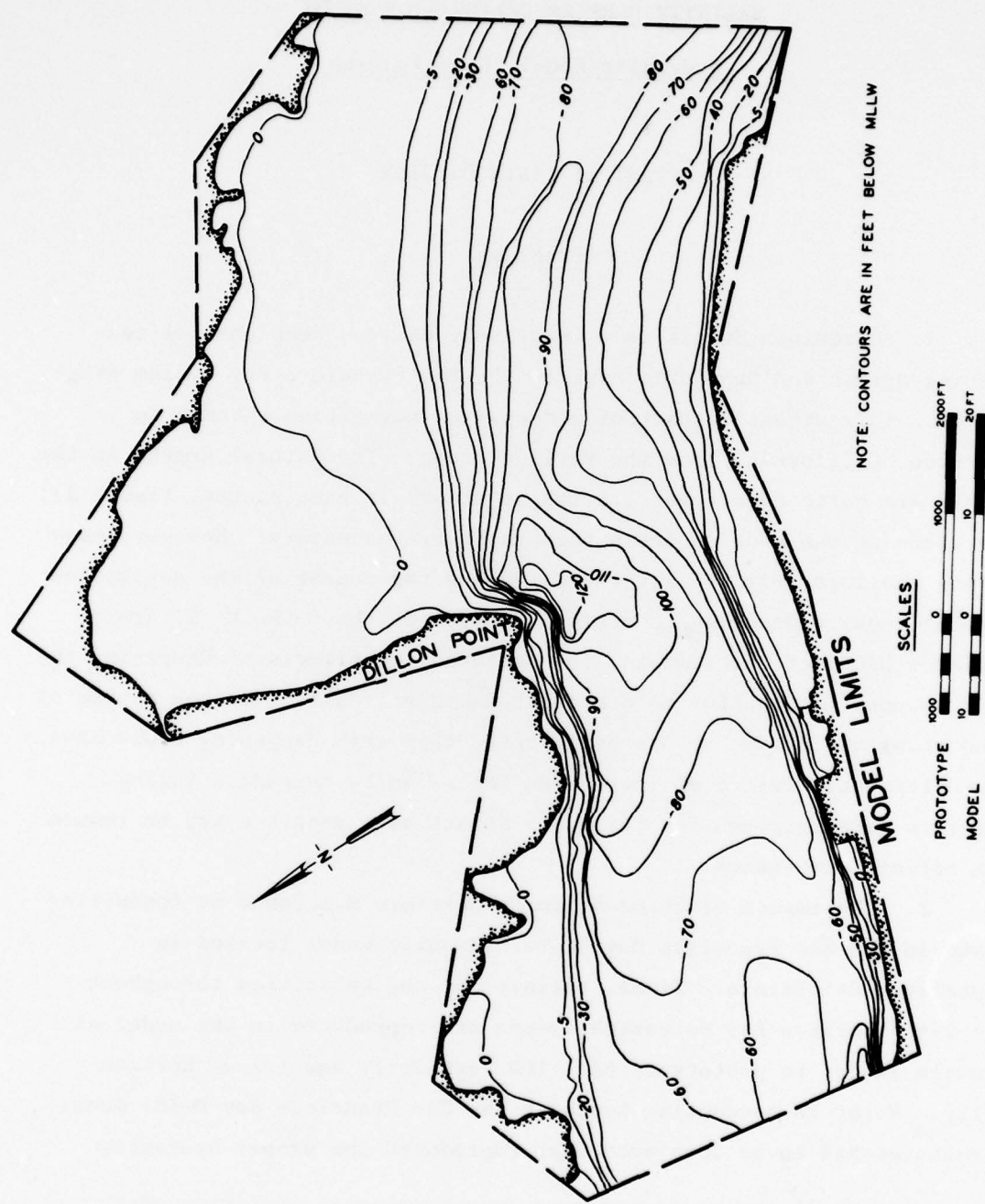


Figure 2. Condition of Carquinez Strait as built in model

characteristics. The most positive method to assume a proper structure is to define the hydraulic characteristics of possible barriers in an undistorted-scale physical model; then by trial-and-error to adjust the geometry of a distorted version of this design barrier until equal water-surface differentials across the structures occur for the same prototype discharge conditions in a model of identical scale as the San Francisco Bay-Delta model.

3. The Sacramento District furnished the U. S. Army Engineer Waterways Experiment Station (WES) the details of three different proposed barrier designs (plans A, B, and C) to be tested in the models. The plan A structure consisted of a sill with a crest width of 12 ft at el -50, with side slopes of 1V on 2H. The plan B structure had a sill width of 12 ft at el -60, with side slopes of 1V on 2H. The plan C structure had a crest elevation of -40 with a crest width of 12 ft and ship lane of 700 ft at el -50, with side slopes of 1V on 2H.

Objective

4. The primary objective of this study was to develop three distorted-scale salinity barriers for use in a comprehensive model of the San Francisco Bay-Delta. In addition, tests were conducted to define the influence of the structures on velocities and flow distribution as they may affect navigation or cause erosion and as the model distortion may affect velocity distribution.

Scope

5. The study consisted of defining the hydraulic characteristics of three proposed salinity barriers, developing the geometry of each scale structure to assure proper hydraulic influence of the structure in the San Francisco Bay-Delta model, and defining the influence of the structures on flow magnitudes and patterns in the immediate vicinity.

PART II: THE MODEL

6. Two fixed-bed models in which steady-state flows in both flood and ebb directions could be reproduced were used in this study. The undistorted-scale model (Figures 3 and 4) reproduced about 2 miles of Carquinez Strait to a linear scale ratio of 1:100. Other scale ratios (model to prototype) were velocity 1:10, discharge 1:100,000, and slope 1:1. The distorted-scale model (Figures 5 and 6) reproduced about 4 miles of Carquinez Strait at the same vertical and horizontal scales (1:100 vertically, 1:1000 horizontally) as the San Francisco Bay-Delta model. Pertinent scale ratios (model to prototype) of this model were velocity 1:10, discharge 1:1,000,000, and slope 10:1. Incorporated in the model was the artificial bend present in the San Francisco Bay-Delta model at Sausalito, California.

7. The models were equipped with the necessary pipes, pumps, flow measurement devices, and water-surface gages to precisely measure the hydraulic characteristics of proposed structure design for either flood or ebb flows.

8. Discharge measurements in both the undistorted- and distorted-scale models were made using venturi meters. The same venturi meters were used for both flood and ebb directions in each model.

9. Measurement of water-surface elevations were made using point gages, graduated to 0.001 ft (0.1 ft prototype). These gages could be read accurately to within ± 0.0005 ft (0.05 ft prototype).

10. Current velocity measurements were made with miniature Price meters. The five-cup meters, constructed of a light plastic material, were approximately 0.04 ft in diameter (4.0 ft prototype) and were mounted on a horizontal wheel about 0.11 ft in diameter (this corresponds to 11 ft prototype for the undistorted-scale model and 110 ft prototype for the distorted-scale model); the center of the cups was 0.05 ft from the bottom of the frame. The meters were calibrated frequently to ensure accurate operation and were capable of measuring actual velocities as low as about 0.03 fps (about 0.3 fps prototype).

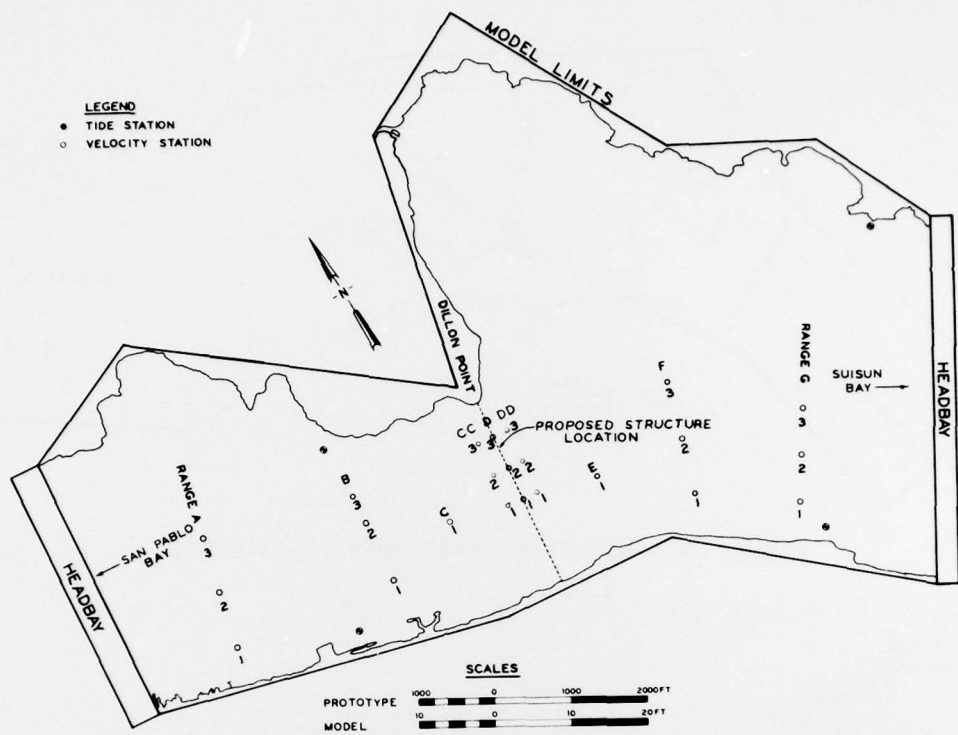


Figure 3. Undistorted-scale model limits map

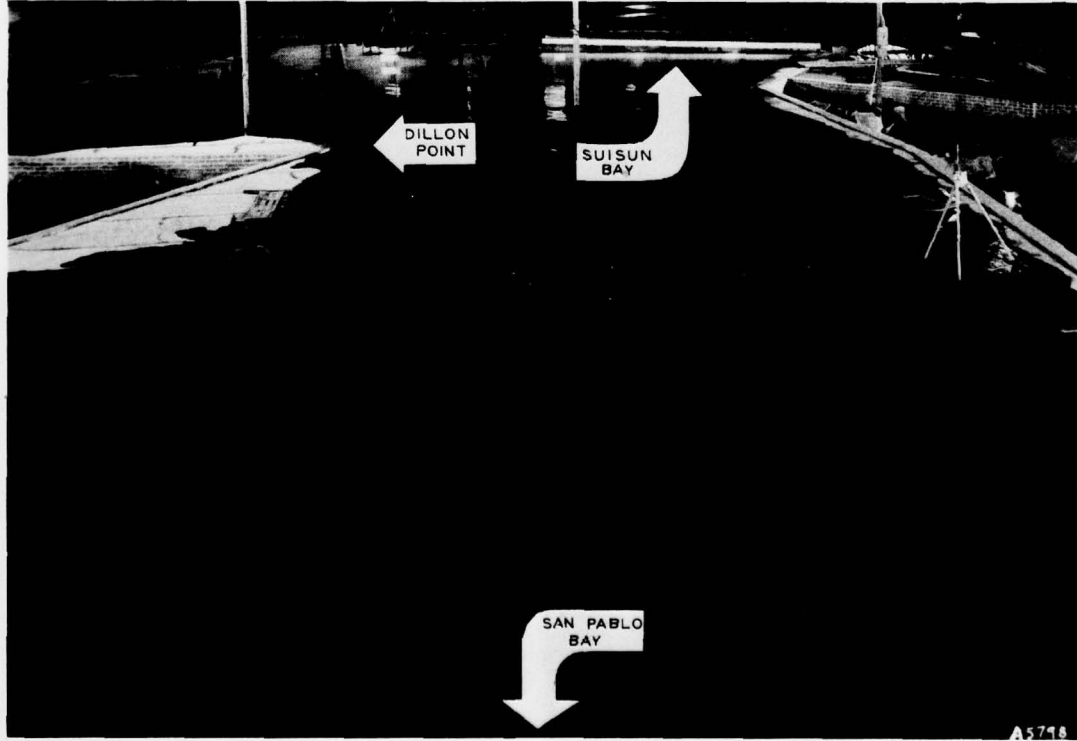


Figure 4. General view of the undistorted-scale model

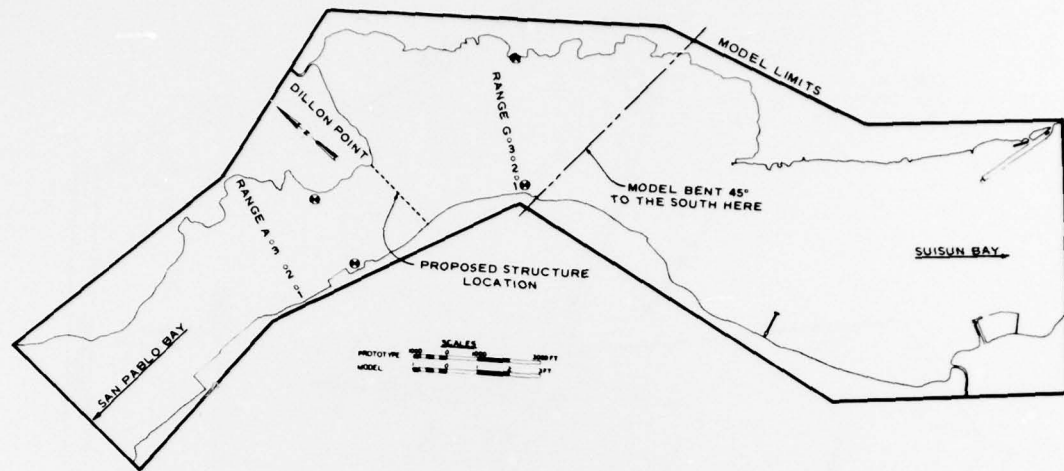


Figure 5. Distorted-scale model limits map



Figure 6. General view of distorted-scale model

11. These models were completely enclosed in a shelter to protect them and their appurtenances from the weather and to permit uninterrupted operation.

PART III: MODEL TESTS AND RESULTS

Description of Tests and Procedures

12. Prior to conducting any tests in the undistorted-scale model, tests were conducted to assure that results from tests in the model would properly represent prototype conditions. These tests are discussed in Appendix A.

13. After proper reproduction of prototype conditions was assured, water-surface profiles were obtained for each proposed structure in the undistorted-scale model at locations shown in Figure 3. Water-surface data were obtained for five discharges ranging from 300,000 to 700,000 cfs in 100,000 cfs increments in both flood and ebb directions. All data were obtained with a headwater elevation of approximately +3.0. These data were recorded independently by three technicians. Since water-surface information from the undistorted-scale model tests was the basis for comparison for all of the trial distorted-structure tests, the data were obtained by establishing the flow in the model for a minimum of two separate occasions. The data used for comparison of trial distorted-scale structures and undistorted-scale structures were the average of combining all readings for the two upstream and then for the two downstream gages for each flow.

14. Once the undistorted-model water-surface data were defined, duplicate tests were conducted in the distorted-scale model for a series of trial structures. These trial structures were selected based on the results of the preceding tests until an acceptable reproduction of the undistorted-scale results was obtained. Gage locations were similar for both undistorted- and distorted-scale tests as shown in Figures 3 and 5. The distorted-scale structure that resulted in the best duplication of the undistorted-scale results was then recommended for use in the comprehensive tests in the San Francisco Bay-Delta model.

15. Adjustments made on the trial distorted structures were limited to changes in crest width and side slopes. Because the structures were to be used in a variable density model, the same crest elevation as

that of the undistorted-scale structure had to be maintained. In addition, the structures had to be designed so they could be easily reproduced in the San Francisco Bay-Delta model. Both undistorted- and distorted-scale structures were molded out of concrete; however, the undistorted-scale structures had a small layer of pea gravel on the outer surface to simulate the size and type of stone considered for use in construction of the prototype.

16. Current velocities were defined in the undistorted-scale model for a discharge of 500,000 cfs in both ebb and flood directions with a headwater elevation of +3.0. Data were obtained at 23 locations (Figure 3) at the surface, 3 ft below the surface, at middepth, and 5 ft above the bottom. After the distorted-scale structure to be used in the San Francisco Bay-Delta model was defined, velocity data were obtained in the distorted-scale model for this structure at range A sta 1-3 and range G sta 1-3 (Figure 5). These data were obtained at the same depths as for the undistorted-scale structure and a discharge of 500,000 cfs.

17. After completing all originally scheduled tests on the three proposed barrier designs, the data indicated that plan A had the greatest effect on velocity distribution of any of the plans. In order to further investigate the potential of plan A to cause bank erosion, surface current patterns for plan A and base conditions were obtained and are shown in Photos 1-8. All photographs were 5-sec time exposures of confetti floating on the water surface. A strobe light was flashed immediately before the camera lens was closed, resulting in a bright spot near the end of each confetti streak to indicate the direction of flow. A scale for converting the total length of the confetti streak to surface current velocity in feet per second (prototype) is provided on each photograph. The velocity value attained in this manner is the average velocity over the 5-sec time span. These photographs were taken for 350,000- and 600,000-cfs discharges in both flood and ebb directions. The headwaters were maintained at el +3.0 for all flows. The photographs are presented here at a reduced scale; however, enlargements of

the original photographs were furnished the Sacramento District and the originals are on file at the WES.

Test Results

18. The Sacramento District furnished WES the details of three different proposed barrier designs (plans A, B, and C) to be tested in the models. These designs were determined by the physical characteristics of the materials to be used and the construction techniques to be followed during actual construction. The following paragraphs discuss the results of model tests of each of the proposed structures.

Plan A

19. The plan A structure consisted of a sill with a crest width of 12 ft at el -50, with side slopes of 1V on 2H (Figure 7). Results

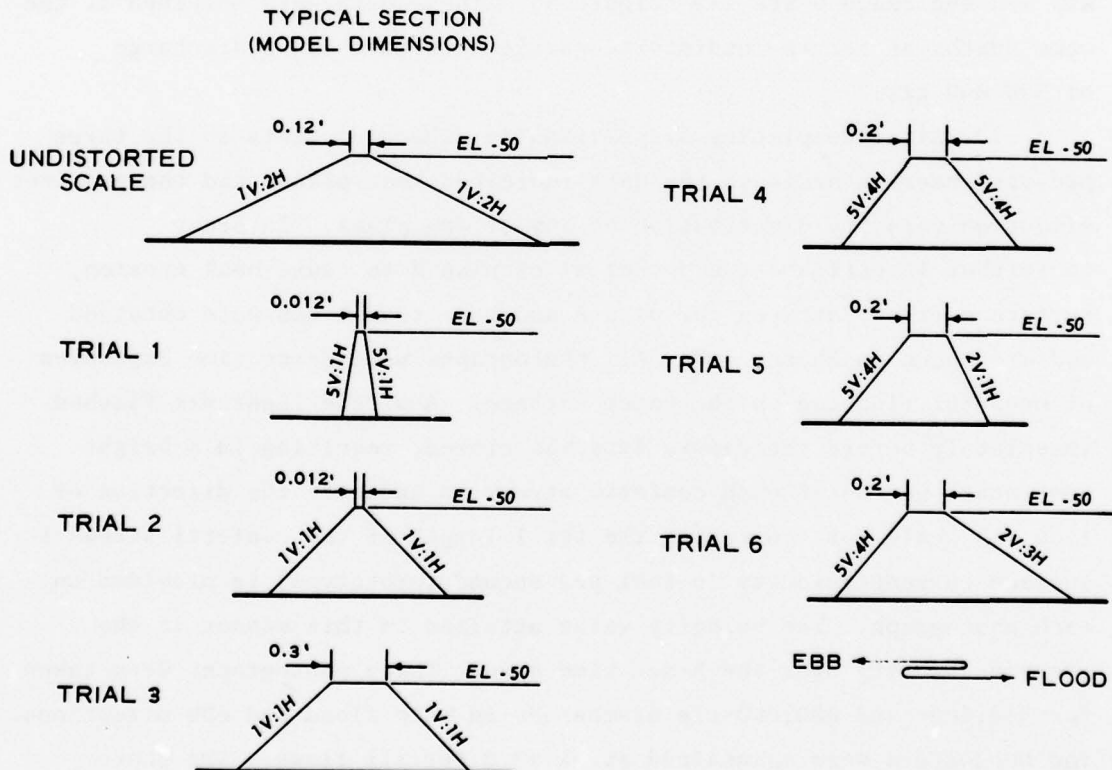


Figure 7. Section views of plan A structures

of undistorted-scale model velocity data are shown in Table 1 and Plates 1-6. The surface currents in both the ebb and flood directions were significantly increased with the structure in place, reaching as high as 6.0 fps along range CC (Table 1). As would be expected, eddies occur on the backside of the structure, and flow at the toe of the structure was in the opposite direction from the mainstream flow as shown in Table 1 by a negative sign preceding the velocity values (Table 1, ranges CC and DD). Bottom velocities were as high as 5.2 fps which occurred in the ebb direction at range D sta 1.

20. A comparison of current velocities for the natural condition and for the plan A condition is shown in Plates 1-6. Changes in velocity measurements between plan A and the natural condition greater than 0.3 fps were considered significant differences, while differences of 0.3 fps or less were considered no change. Plan A, which reduced the natural cross section by 47 percent (at mllw), significantly increased current velocities at the structure location and had some effect on the velocity patterns at more distant velocity stations. In the flood direction, surface current velocities west (upcurrent) from the barrier tended to increase at stations on the north side of the channel and to be reduced on the south side for stations west of the structure. However, east (downcurrent) of the structure the reverse was true with velocities at stations near the inside of the bend (south side) being increased. The pattern of velocity changes at middepth were similar to those at the surface, except the magnitude of the change was generally lower. At the bottom, the pattern of change was reversed west of the structure and similar east of the structure. Along the bottom all velocities were increased by the structure. In the ebb direction, current velocity changes generally were similar for surface, middepth, and bottom elevations. East (upcurrent) of the structure (approach), velocities were increased at stations on the south side of the channel. West (downcurrent) of the structure, increases occurred at stations on the south side of the channel with a decrease in velocities in the center and north side for the surface and middepth. Minimal changes occurred near the bottom.

21. Photos 1-8 show that plan A caused high velocities to occur adjacent to the north and south end of the sill and could cause scour of the shore in these locations. The eddy formation along the south shore adjacent to Dillon Point (Photo 7) was decreased in size and moved approximately 600 ft upstream (Photo 8) during ebb flow with the plan A sill.

22. In the course of conducting the study, concern developed that the increased current velocities near the structure would pose a navigation problem. For this reason, tests with a 1:100-scale ship model were conducted in the Carquinez Strait undistorted-scale model. The scale model ship simulated a tanker 565 ft long, 85 ft wide, 33 ft draft, and 33,000-dwt displacement (shown in the model in Figure 8). The tests



Figure 8. Tanker model crossing plan A sill

were conducted with a flow of 500,000 cfs (prototype) in the ebb direction with the plan A structure in place. The remote-controlled model

ship made several passes over the structure, both upstream and downstream, with no apparent difficulties.

23. The geometry of each trial distorted-scale structure is shown in Figure 7. A comparison of water-surface differentials for a range of discharges is shown in Figure 9 for the undistorted-scale model of Carquinez Strait with plan A and the various trial distorted-scale structures. Calibration of a structure to represent plan A in a distorted-scale model was accomplished by adjustment to each successive trial structure until agreement between the trial structure and the desired undistorted-scale-plan A structure was reached. The first trial was the geometrically scaled structure, which produced water-surface differentials much too large, particularly in the ebb direction. More gentle side slopes and, eventually, wider crest widths were used until a satisfactory comparison was achieved by trial 4. Further attempts, trials 5 and 6, did not produce any significant improvement with trial 5 about equal to trial 4. Trial 4 was selected as the distorted-scale plan A structure, and the necessary velocity data in the distorted-scale model were then obtained (Table 2).

24. The lateral distribution of velocities along ranges A and G are somewhat different in the undistorted- and distorted-scale models for plan A. For both ranges at flood and ebb flow for this discharge, the maximum velocities in the undistorted-scale model were at sta 1 or toward the south side of the strait. However, the distorted-scale model with the artificial bend was unable to reproduce this distribution due to exaggeration of the effects of natural bends on velocity distribution resulting from a radius of curvature of 1/10 of the undistorted-scale model with identical velocity scales and more pronounced boundary effects from the sides of the channel. Instead, the maximum velocities tended to be toward the center of the channel.

25. The average surface, middepth, and bottom velocities for an entire range are also shown in Table 2. The averaging of velocities for one depth across the entire range minimizes the difference in lateral distribution so that the vertical velocity profile can be studied. Energy losses in the distorted-scale model have to occur in one-tenth

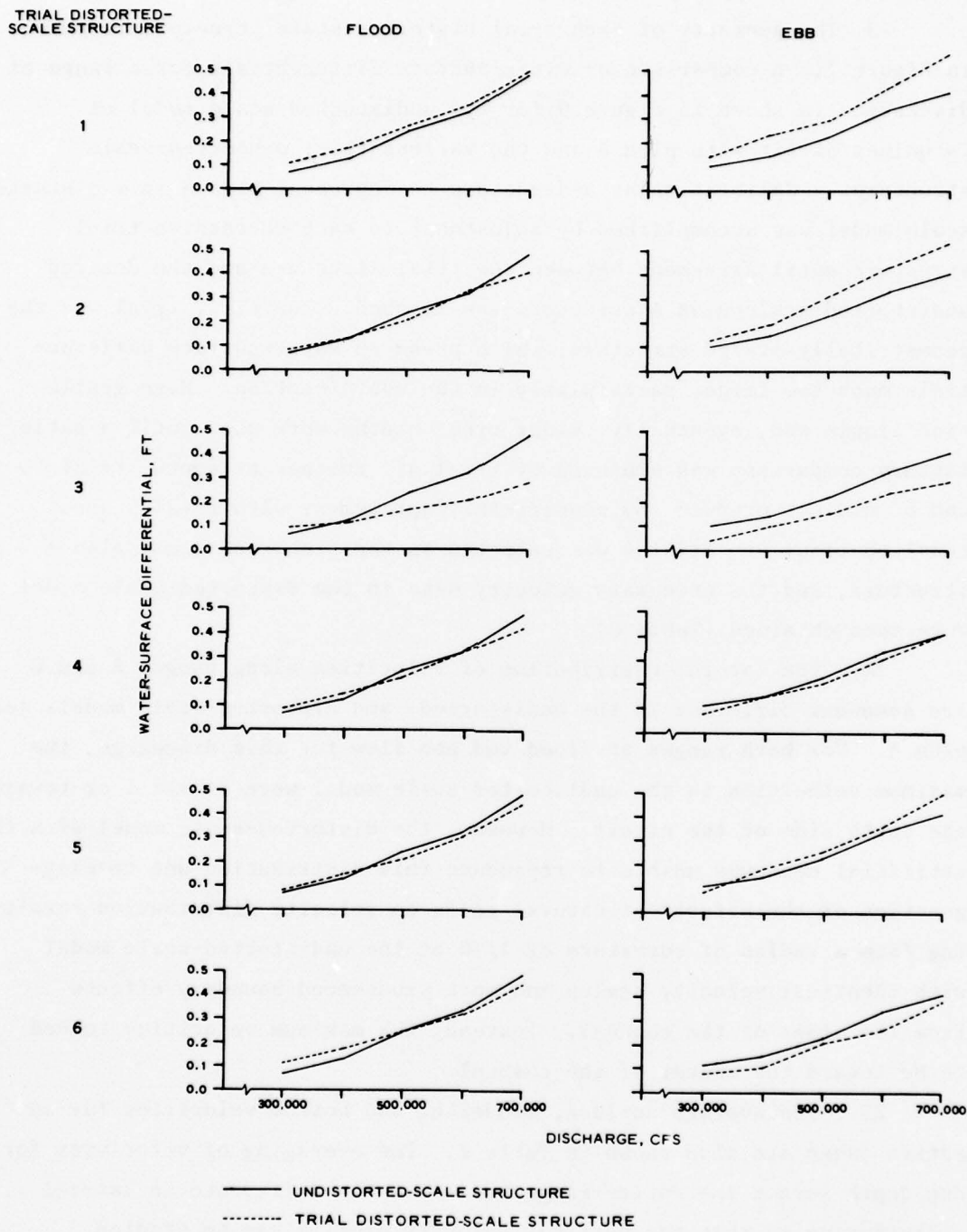


Figure 9. Plan A water-surface differentials

the distance required for the undistorted-scale model; these rapid energy losses are obtained by increased turbulence generated by proper selection of the shape of the distorted-scale structure. The velocity distribution near hydraulically similar distorted- and undistorted-scale structures will not be identical; at some point farther away from the structure, the vertical velocity profile should be reestablished. Ranges A and G were near the upstream and downstream limits of the undistorted-scale model and so were selected as the velocity ranges for the undistorted- and distorted-scale model comparison. Figure 10 shows

RANGE

FLOOD

EBB

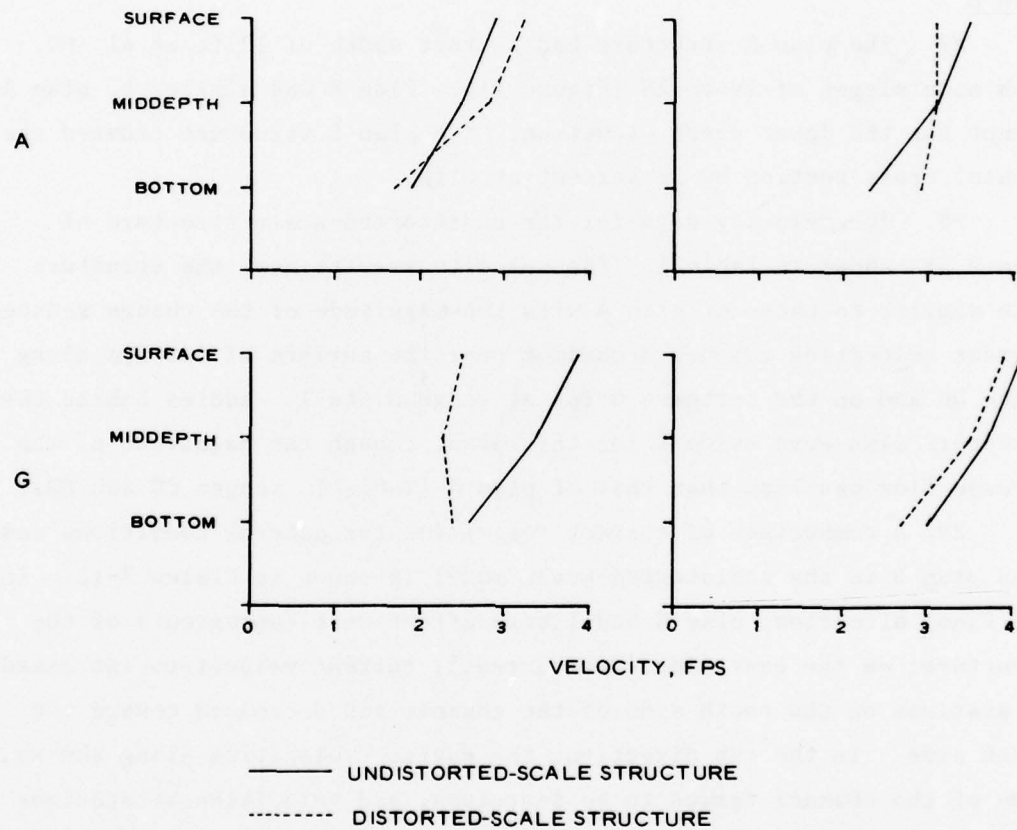


Figure 10. Vertical velocity profiles for undistorted- and distorted-scale plan A structures

that the undistorted-scale model for both ranges and in both flood and ebb directions had a typical vertical velocity profile (logarithmic)

with the greatest velocity near the surface. The distorted-scale model had quite similar profiles for the range that was on the approach side of the structure (range A in the flood direction and range G in the ebb direction). However, the ranges on the opposite side of the structure had velocity profiles that were nearly vertical; i.e., the surface, mid-depth, and bottom velocity values were about the same. For this particular flow, the near-field velocity effects of the distorted-scale plan A structure were observed at the model limits.

26. The reduction in discharge caused by the plan A sill (steady-state compared with tidal mode) is shown in Appendix B.

Plan B

27. The plan B structure had a crest width of 12 ft at el -60, with side slopes of 1V on 2H (Figure 11). Plan B was similar to plan A except for the lower crest elevation. The plan B structure reduced the natural cross section by 38 percent at mllw.

28. The velocity data for the undistorted-scale structure of plan B are shown in Table 1. The velocity results near the structure were similar to those of plan A with the magnitude of the change reduced. Current velocities reached a maximum near the surface of 4.8 fps along range DD and on the bottom 4.0 fps at range D sta 1. Eddies behind the structure also were evident for this plan, though the magnitude of the reverse flow was less than that of plan A (Table 1, ranges CC and DD).

29. A comparison of current velocities for natural conditions and with plan B in the undistorted-scale model is shown in Plates 7-12. In the flood direction, plan B had little effect west (upcurrent) of the structure; on the east side (downcurrent), current velocities increased at stations on the south side of the channel and decreased toward the north side. In the ebb direction, the surface velocities along the south side of the channel tended to be increased, and velocities at stations toward the north side were slightly decreased. The middepth velocities exhibited these changes only west (downcurrent) of the structure, while bottom velocities were not significantly affected except near the surface.

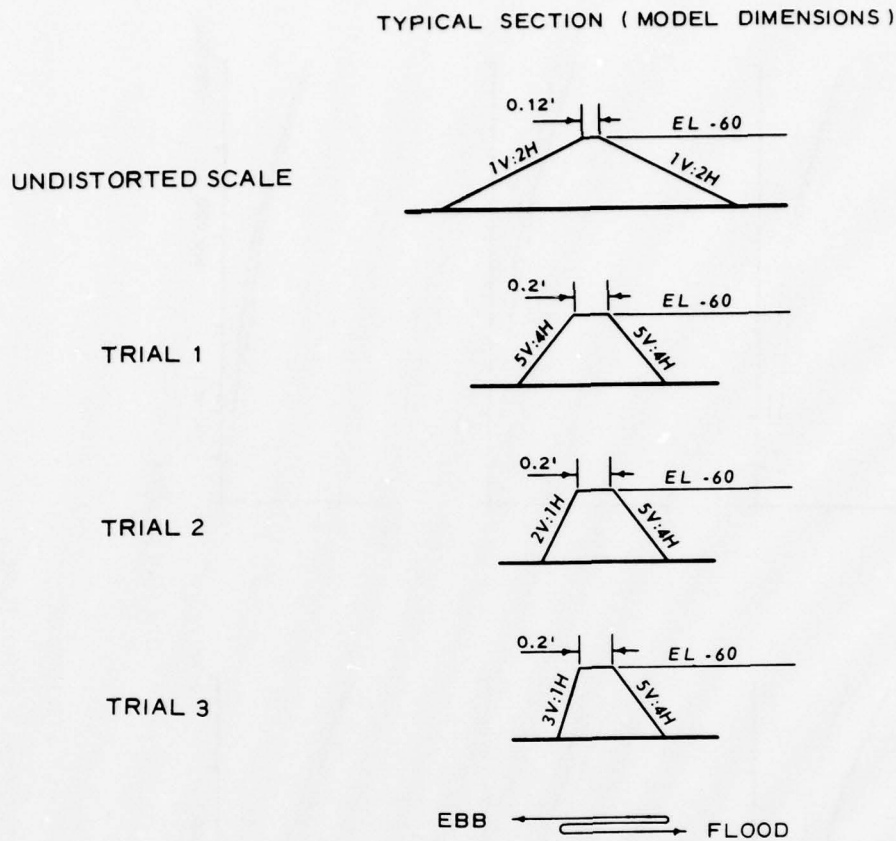


Figure 11. Section view of plan B trial distorted-scale structures

30. The geometry of each trial distorted-scale structure is shown in Figure 11. The comparison of water-surface differentials for a range of discharges for the undistorted-scale version of plan B along with the trial distorted-scale structures is shown in Figure 12. The first trial distorted-scale structure used for plan B was similar to that which was successful for plan A. The comparison in the ebb direction was good, but this structure was too efficient in the flood direction. The downstream side slope (side of the structure toward the ocean) was steepened until satisfactory agreement was achieved. Trial 3 structure was designated the distorted-scale plan B structure to be used in the San Francisco Bay-Delta model at Sausalito, California. Results of

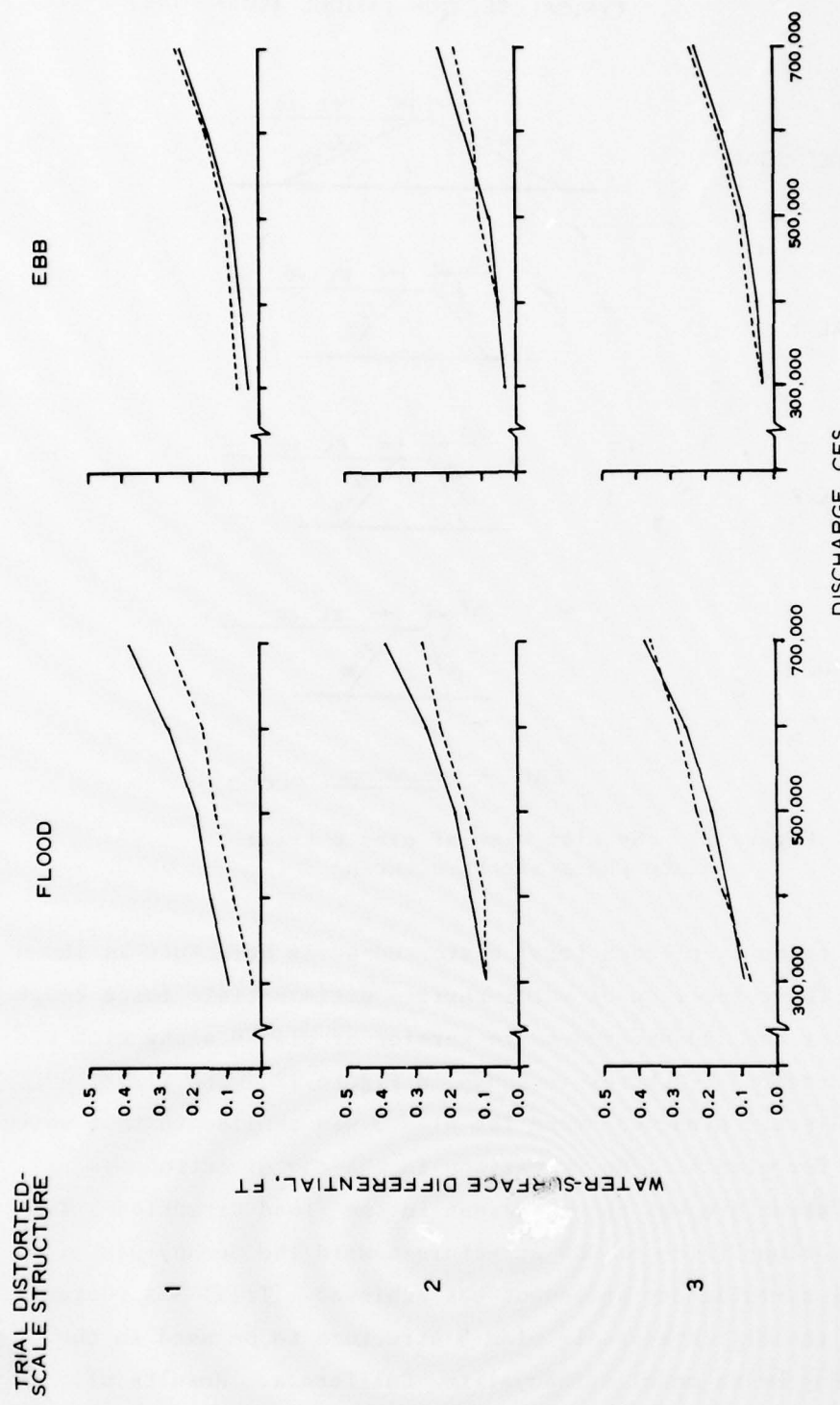


Figure 12. Plan B water-surface differentials

current velocity measurements made in the distorted-scale model with this structure in place are shown in Table 2.

31. Comparison of horizontal distribution of velocities in the distorted- and undistorted-scale plan B structures was similar to that for plan A. Maximum velocities for the undistorted-scale model were toward the south side of the channel, whereas in the distorted-scale model the maximum velocities tended to be toward the middle of the channel. The vertical velocity profiles for this plan (Figure 13) are again quite like those of plan A; the velocity profiles for the distorted-scale

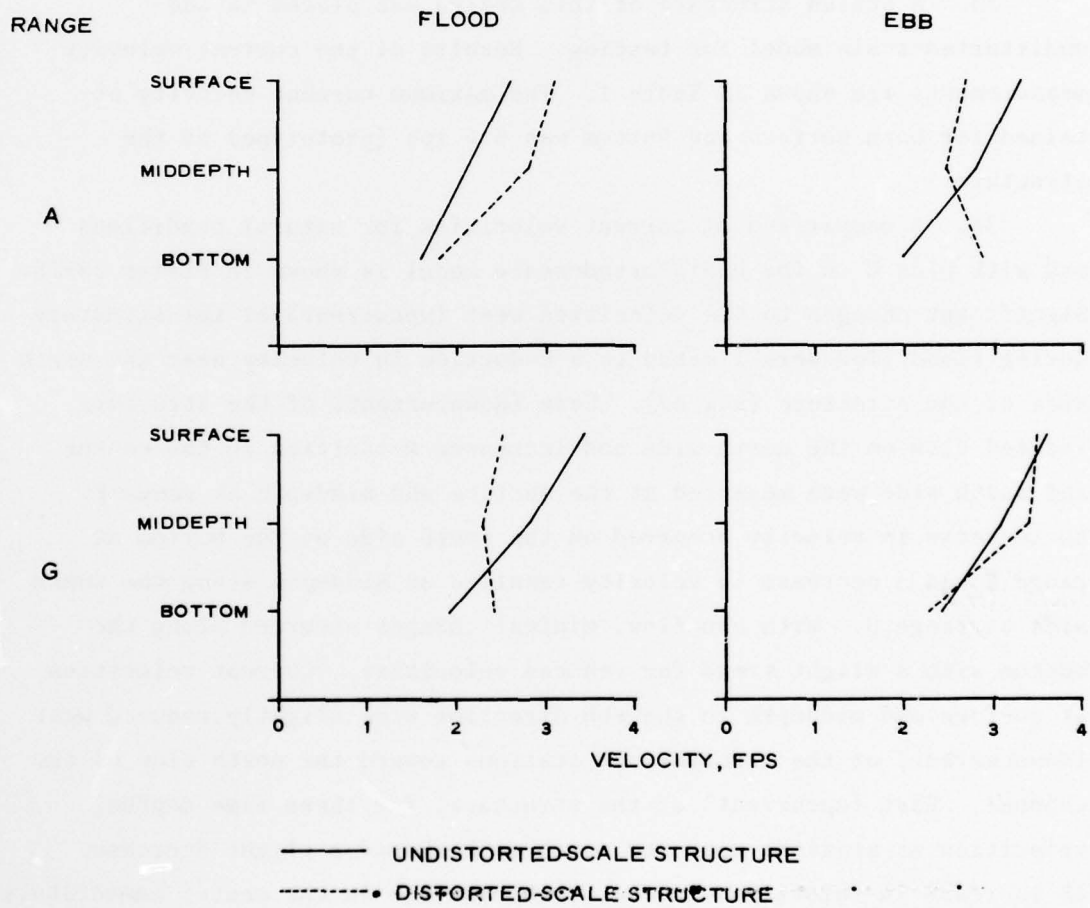


Figure 13. Vertical velocity profiles for undistorted- and distorted-scale plan B structures

model on the approach side of the structure are comparable to those of the undistorted-scale model. The profiles on the opposite side of the structure are still within the near-field velocity effects of the distorted structure at the model limits.

Plan C

32. The final proposed barrier design tested, designated as plan C (Figure 14), had a crest elevation of -40 with a crest width of 12 ft and ship lane of 700 ft at el -50. All slopes for this barrier were 1V on 2H. This plan reduced the natural cross section by 53 percent.

33. A scaled structure of this design was placed in the undistorted-scale model for testing. Results of the current velocity measurements are shown in Table 1. The maximum current velocity attained for both surface and bottom was 5.4 fps (prototype) at the structure.

34. A comparison of current velocities for natural conditions and with plan C in the undistorted-scale model is shown in Plates 13-18. Significant changes to the velocities west (upcurrent) of the structure during flood flow were limited to a reduction in velocity near the north side of the structure (sta B3). East (downcurrent) of the structure, reduced flow on the north side and increased velocities in the center and south side were measured at the surface and middepth at range F. An increase in velocity occurred on the south side on the bottom at range F and a decrease in velocity resulted at middepth along the south side at range G. With ebb flow, minimal changes occurred along the bottom with a slight trend for reduced velocities. Current velocities at surface and middepth in the ebb direction were slightly reduced west (downcurrent) of the structure at stations toward the north side of the channel. East (upcurrent) of the structure, for these same depths, velocities at stations near the south bank showed a slight decrease. An increase in velocity occurred at the surface in the center immediately east of the structure and along the north side at middepth.

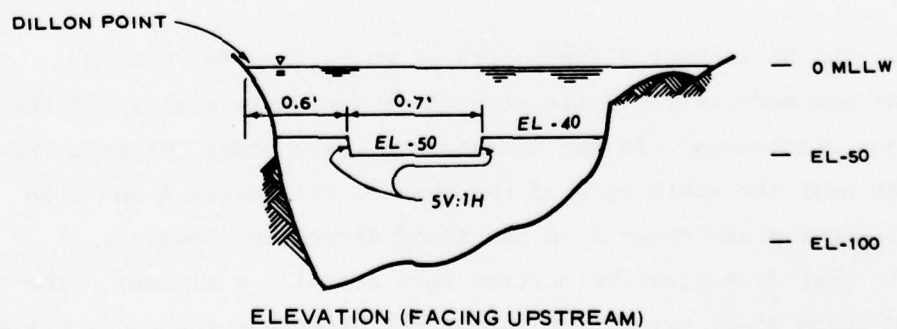
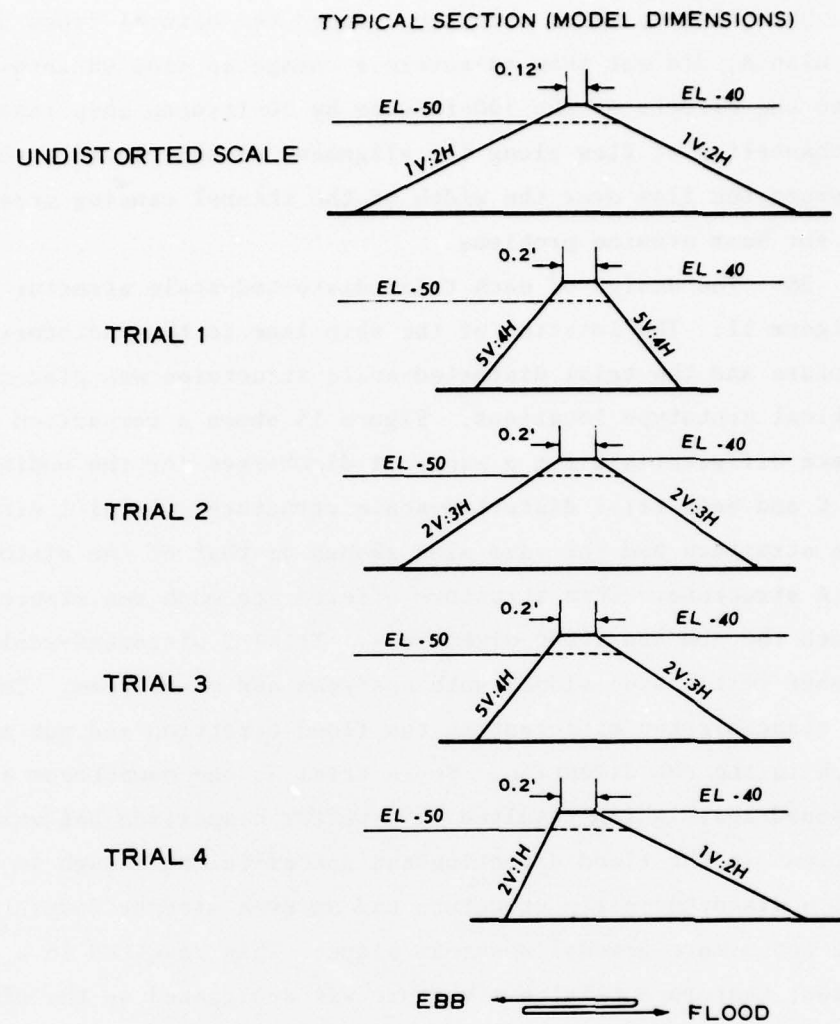


Figure 14. Geometry of plan C structures

35. Plan C, which actually reduced the natural cross section more than plan A, did not show as severe a change in flow patterns. This was due to the effects of the 700-ft-wide by 50-ft-deep ship lane maintaining the channeling of flow along the alignment of the channel, whereas plan A dispersed the flow over the width of the channel causing greater potential for bank erosion problems.

36. The design of each trial distorted-scale structure is shown in Figure 11. The location of the ship lane in the undistorted-scale structure and the trial distorted-scale structures was placed in identical prototype locations. Figure 15 shows a comparison of water-surface differentials for a range of discharges for the undistorted-scale plan C and each trial distorted-scale structure. Trial 1 distorted-scale structure had the same side slopes as that of the distorted-scale plan A structure. This structure offered too much resistance to flow in both the ebb and flood directions. Trial 2 distorted-scale structure had more gentle side slopes both upstream and downstream. This resulted in a structure too efficient in the flood direction and not efficient enough in the ebb direction. So in trial 3, the downstream slope was steepened again which resulted in a better comparison but was still too efficient in the flood direction and not efficient enough in the ebb. Trial 4 distorted-scale structure had an even steeper downstream side slope and a more gradual upstream slope. This resulted in a good comparison; therefore trial 4 structure was designated as the distorted-scale plan C structure. Results of current velocity measurements made in the distorted-scale model with this structure in place are shown in Table 2.

37. The horizontal distribution of velocities for plan C distorted- and undistorted-scale structures was quite similar to that of previous structures. In the undistorted-scale model, maximum velocities were near the south side of the channel for ranges A and G in the ebb direction and range A in the flood direction; however, at range G in that direction, velocities were actually a minimum. The distorted-scale model velocities in the ebb direction reached a maximum at the center of the channel. The distorted-scale model had

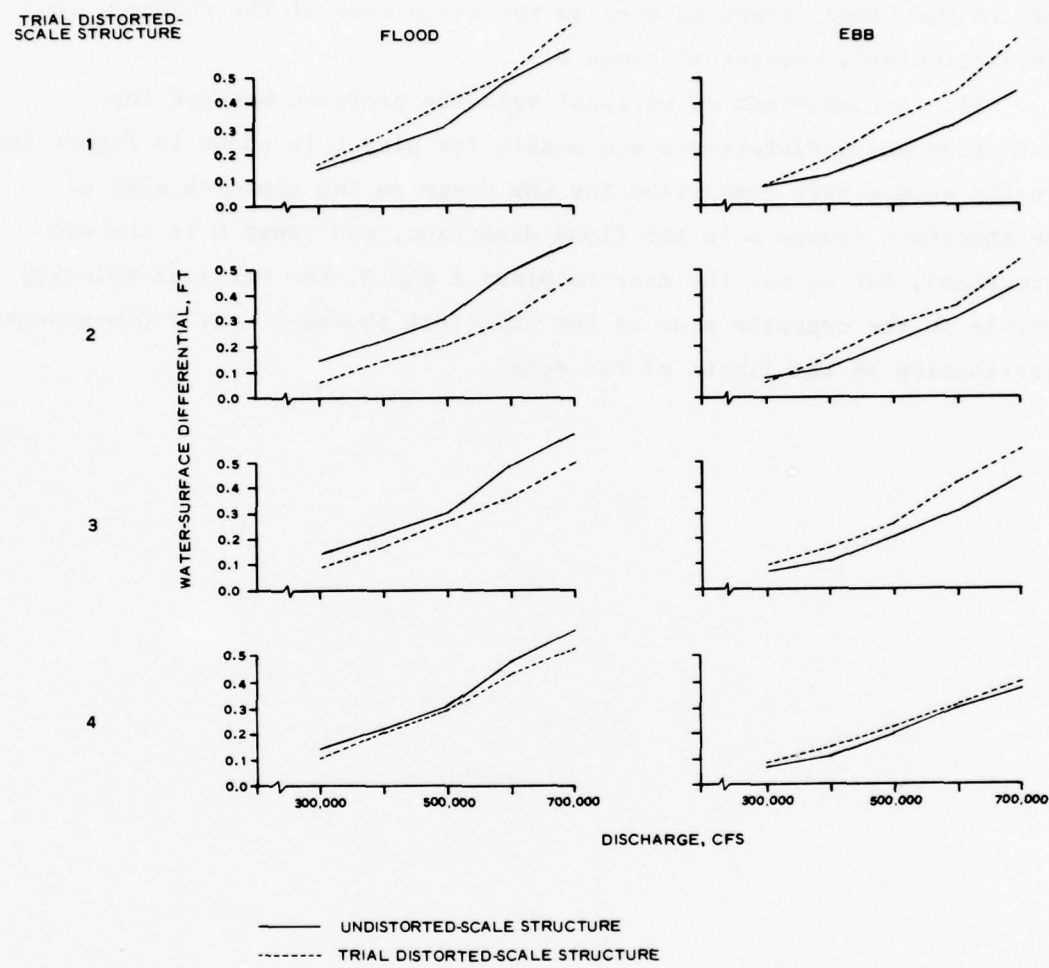


Figure 15. Plan C water-surface profiles

significantly higher velocities than the undistorted-scale model at the center stations in the ebb direction. The distorted-scale model velocities in the flood direction were on the north side of the channel; this was particularly evident at range G.

38. A comparison of vertical velocity profiles between the distorted- and undistorted-scale models for plan C is shown in Figure 16. Results show a fair comparison for the range on the approach side of the structure (range A in the flood direction, and range G in the ebb direction), but as was the case in plans A and B, the vertical velocity profile on the opposite side of the structure showed a nearly homogeneous distribution at the limits of the model.

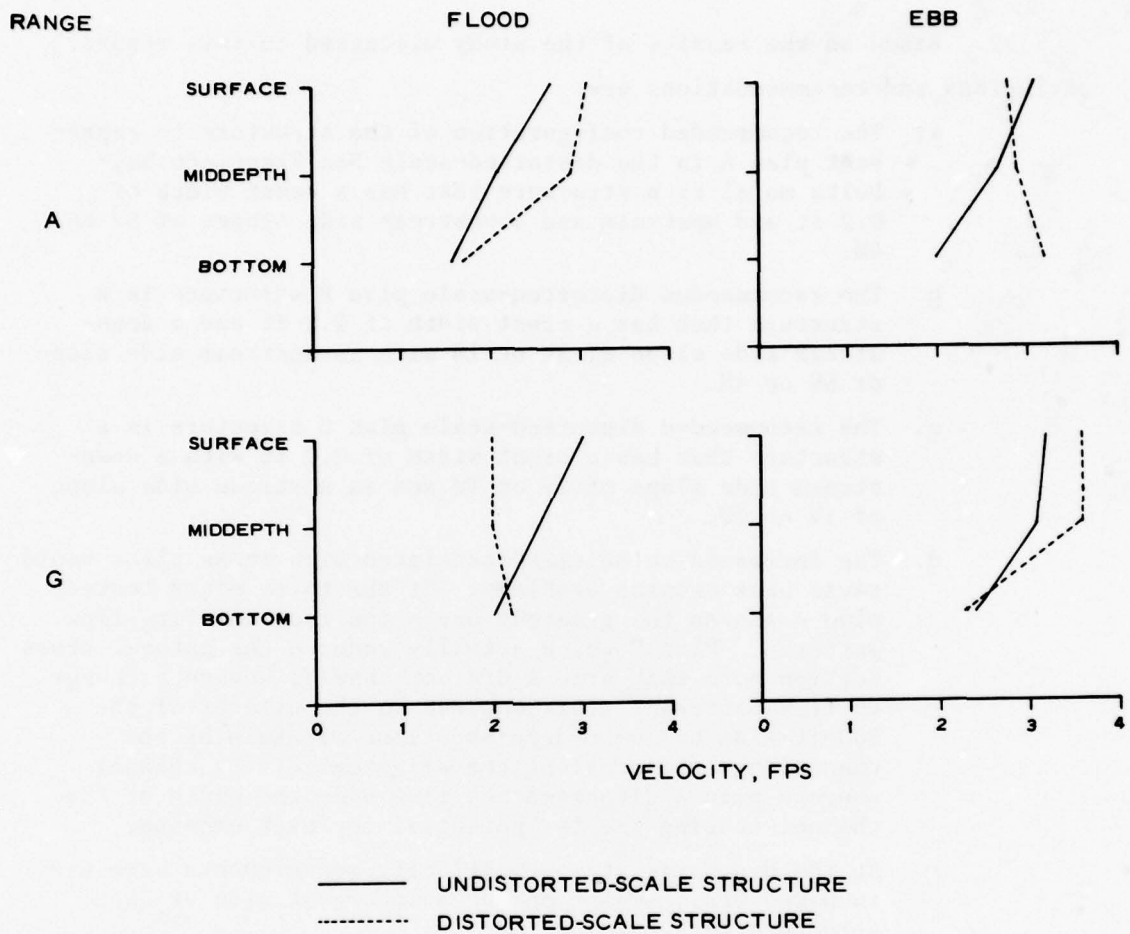


Figure 16. Vertical velocity profiles for undistorted- and distorted-scale plan C structures

PART IV: CONCLUSIONS AND RECOMMENDATIONS

39. Based on the results of the study discussed in this report, conclusions and recommendations are:

- a. The recommended configuration of the structure to represent plan A in the distorted-scale San Francisco Bay-Delta model is a structure that has a crest width of 0.2 ft and upstream and downstream side slopes of 5V on 4H.
- b. The recommended distorted-scale plan B structure is a structure that has a crest width of 0.2 ft and a downstream side slope of 3V on 1H with an upstream side slope of 5V on 4H.
- c. The recommended distorted-scale plan C structure is a structure that has a crest width of 0.2 ft with a downstream side slope of 2V on 1H and an upstream side slope of 1V on 2H.
- d. The increased velocities associated with these plans could cause bank erosion problems. Of the three plans tested, plan A showed the greatest deviation from existing flow patterns. Plan C which actually reduced the natural cross section more than plan A did not show as severe a change in flow patterns. This was due to the effects of the 700-ft-wide by 50-ft-deep ship lane maintaining the channeling of flow along the alignment of the channel, whereas plan A dispersed the flow over the width of the channel causing greater potential for bank erosion.
- e. At the discharge at which velocity measurements were made (500,000 cfs), eddies on the downcurrent side of each structure were evident.
- f. The velocity distribution measured in the undistorted-scale model near the model boundaries (4,000 ft from the structure in the ebb direction and 3,500 ft from the structure in the flood direction) could not be reproduced in the distorted-scale section model because of the model distortion and the artificial bend located near the site of the structure. The influence of the structures on velocity distribution will not be reproduced near the structures in the San Francisco Bay-Delta model; however, the lack of velocity reproduction does not affect the reproduction of the proper flow through each structure in the San Francisco Bay-Delta model.

Table 1
Velocities for Plans A, B, and C
Undistorted-Scale Structures for 500,000-cfs Discharge

Range	Sta	Depth	Velocity, fps							
			Base		Plan A		Plan B		Plan C	
			Flood	Ebb	Flood	Ebb	Flood	Ebb	Flood	Ebb
A	1	Surface	3.8	3.1	3.7	4.4	3.4	3.8	3.8	3.3
		Middepth	2.4	2.8	2.7	3.9	2.4	3.3	2.3	2.9
		Bottom	1.5	2.1	2.0	2.8	1.3	2.4	1.6	2.3
A	2	Surface	2.4	3.2	1.5	3.2	1.9	3.1	2.0	3.2
		Middepth	1.6	2.8	1.9	2.8	1.8	2.6	1.6	2.8
		Bottom	1.0	2.2	1.7	2.1	1.6	1.9	1.4	2.0
A	3	Surface	2.4	3.2	3.5	2.8	2.4	3.0	2.4	2.8
		Middepth	2.1	3.0	2.8	2.5	2.2	2.4	2.3	2.4
		Bottom	1.8	2.1	1.9	2.0	1.8	1.8	1.9	1.8
B	1	Surface	2.9	2.8	2.5	4.2	2.4	3.6	2.8	2.9
		Middepth	2.6	2.8	2.7	3.9	2.2	3.4	2.3	2.9
		Bottom	1.9	2.1	2.3	3.2	1.6	2.4	1.8	2.3
B	2	Surface	3.0	3.2	2.7	2.5	2.8	2.9	2.8	3.1
		Middepth	2.8	3.0	2.8	2.5	2.6	2.4	2.4	2.8
		Bottom	2.1	2.3	2.5	2.0	1.9	2.1	1.6	2.3
B	3	Surface	3.0	3.2	3.5	2.4	3.0	2.8	2.2	2.4
		Middepth	2.6	2.8	3.2	2.3	2.4	2.2	2.6	2.2
		Bottom	2.0	1.8	2.7	2.0	1.6	1.6	1.8	2.0
C	1	Surface	2.4	2.8	2.8	3.4	2.4	2.4	2.6	2.8
		Middepth	2.0	2.4	2.7	2.9	2.2	2.2	2.1	2.1
		Bottom	1.2	1.6	2.0	2.5	1.6	1.6	1.8	2.1
CC	1	Surface	2.2	2.8	2.7	5.9	2.7	4.5	2.8	5.2
		Middepth	1.8	2.6	2.5	2.1	2.5	3.2	2.4	2.1
		Bottom	1.2	2.0	2.0	-1.9	1.8	-1.2	1.9	-1.3
CC	2	Surface	2.8	3.3	2.8	5.6	2.8	4.8	2.9	4.8
		Middepth	2.8	2.8	2.7	1.7	2.2	1.8	2.4	2.4
		Bottom	1.9	1.9	1.4	-1.2	1.4	-1.0	1.4	-1.4
CC	3	Surface	3.3	3.1	2.4	6.0	3.1	4.4	3.0	5.0
		Middepth	2.9	2.6	2.8	1.3	2.4	1.8	2.2	1.2
		Bottom	2.2	1.5	0.9	-1.3	0.9	-1.1	0.8	-1.2
D	1	Surface	2.0	3.0	4.4	5.2	4.0	4.2	5.1	5.1
		Middepth	2.0	2.6	4.5	5.1	3.6	3.8	5.2	5.2
		Bottom	1.4	2.0	4.4	5.2	4.0	3.8	5.4	5.4

(Continued)

Table 1 (Concluded)

Range	Sta	Depth	Velocity, fps							
			Base		Plan A		Plan B		Plan C	
			Flood	Ebb	Flood	Ebb	Flood	Ebb	Flood	Ebb
D	2	Surface	2.8	3.3	4.8	4.9	4.2	4.2	4.9	5.1
		Middepth	2.8	3.0	4.8	4.9	3.8	4.4	4.8	5.3
		Bottom	1.7	2.1	4.8	5.1	3.4	3.2	4.9	4.9
D	3	Surface	3.3	3.1	4.8	4.8	4.4	3.8	5.4	5.0
		Middepth	3.1	2.6	4.7	4.7	3.8	3.6	5.2	5.2
		Bottom	1.7	1.7	4.1	4.8	3.8	3.4	5.4	4.8
DD	1	Surface	2.2	3.2	5.1	3.7	4.2	3.2	5.1	2.8
		Middepth	2.0	2.8	3.1	3.3	2.5	2.7	1.9	2.9
		Bottom	1.6	2.2	-1.2	1.7	-0.9	2.2	-1.6	1.9
DD	2	Surface	3.0	3.3	5.3	3.1	4.8	3.4	4.9	2.8
		Middepth	2.8	3.0	1.9	2.8	2.2	2.2	2.6	2.4
		Bottom	2.1	1.7	-1.5	1.2	-1.0	1.2	-1.3	1.8
DD	3	Surface	3.3	2.9	5.5	2.9	4.8	2.6	5.2	2.4
		Middepth	3.1	2.6	1.9	2.4	1.4	2.3	1.2	2.2
		Bottom	1.7	1.5	-1.6	1.2	-1.1	1.1	-1.0	0.8
E	1	Surface	3.2	4.1	3.7	4.8	3.2	4.0	3.4	4.2
		Middepth	3.0	3.7	3.5	4.2	3.2	3.4	2.8	3.2
		Bottom	2.4	2.8	3.0	3.1	2.9	2.7	2.2	2.4
F	1	Surface	3.7	3.7	5.3	4.9	4.2	4.5	4.6	3.3
		Middepth	3.3	3.8	4.7	4.3	4.2	3.8	4.8	3.4
		Bottom	2.4	2.8	3.7	3.3	2.9	2.9	3.6	2.8
F	2	Surface	3.1	2.6	3.9	2.9	3.4	2.4	3.6	3.8
		Middepth	2.8	3.3	3.5	3.8	2.9	3.1	3.2	3.2
		Bottom	1.9	2.3	2.7	3.1	2.1	2.3	2.0	2.2
F	3	Surface	3.6	3.0	2.3	3.1	2.2	2.6	2.3	2.9
		Middepth	2.8	2.2	2.3	2.9	2.2	2.4	2.3	2.6
		Bottom	1.8	1.8	1.9	2.3	1.8	1.8	1.8	2.1
G	1	Surface	2.8	4.4	4.8	4.9	3.8	4.4	2.6	4.3
		Middepth	2.4	4.2	3.9	4.5	3.1	3.8	1.9	3.8
		Bottom	1.6	3.3	3.1	3.7	2.1	2.8	1.9	2.9
G	2	Surface	3.2	3.3	3.5	4.0	3.3	3.4	3.1	2.3
		Middepth	2.8	3.2	3.2	3.6	2.8	2.9	2.8	2.9
		Bottom	2.1	2.3	2.7	3.1	1.9	2.6	2.1	2.6
G	3	Surface	3.4	3.2	3.3	3.5	3.0	3.0	3.2	3.0
		Middepth	2.6	2.6	3.1	3.1	2.4	2.6	2.8	2.6
		Bottom	1.8	2.2	1.9	2.1	1.8	1.8	2.0	1.8

Table 2
 Velocities at Ranges A and G for Undistorted- and Distorted-Scale Structures
 for 500,000-cfs Discharge

Range	Station	Depth	Plan A				Plan B				Plan C			
			Flood		Ebb		Flood		Ebb		Flood		Ebb	
			u.s.*	d.s.4*	u.s.	d.s.4	u.s.	d.s.3	u.s.	d.s.3	u.s.	d.s.4	u.s.	d.s.4
A	1	Surface	3.7	2.6	4.4	2.4	3.4	2.6	3.8	2.8	3.8	2.4	3.3	2.2
		Middepth	2.7	2.4	3.9	2.8	2.4	2.2	3.3	2.6	2.3	2.8	2.9	2.8
		Bottom	2.0	1.8	2.8	2.6	1.3	1.8	2.4	2.4	1.6	1.8	2.3	2.8
A	2	Surface	1.5	3.4	3.2	3.8	1.9	3.4	3.1	3.0	2.0	3.4	3.2	4.2
		Middepth	1.9	3.0	2.8	3.6	1.8	3.0	2.6	2.6	1.6	3.0	2.8	4.4
		Bottom	1.7	1.8	2.1	3.6	1.6	2.0	1.9	3.6	1.4	1.8	2.0	4.2
A	3	Surface	3.5	3.6	2.8	3.0	2.4	3.4	3.0	2.4	2.4	3.4	2.8	2.0
		Middepth	2.8	3.0	2.5	2.8	2.2	3.2	2.4	2.4	2.3	3.0	2.4	1.6
		Bottom	1.9	1.6	2.0	2.6	1.8	1.6	1.8	2.6	1.9	1.6	1.8	2.6
A	Average	Surface	2.9	3.2	3.5	3.1	2.6	3.1	3.3	2.7	2.7	3.1	3.1	2.8
		Middepth	2.5	2.8	3.1	3.1	2.1	2.8	2.8	2.5	2.1	2.9	2.7	2.9
		Bottom	1.9	1.7	2.3	2.9	1.6	1.8	2.0	2.0	1.6	1.7	2.0	3.2
G	1	Surface	4.8	1.6	4.9	3.9	3.8	1.8	4.4	3.4	2.6	1.4	4.3	3.6
		Middepth	3.9	2.3	4.5	3.6	3.1	2.4	3.8	3.6	1.9	1.6	3.8	3.9
		Bottom	3.1	2.3	3.7	2.4	2.1	1.9	2.8	2.8	1.9	1.1	2.9	2.8
G	2	Surface	3.5	2.8	4.0	4.1	3.3	3.1	3.4	3.9	3.1	2.8	2.1	2.3
		Middepth	3.2	2.6	3.6	3.4	2.8	2.4	2.9	3.3	2.3	2.1	2.9	4.4
		Bottom	2.7	2.1	3.1	2.3	1.9	2.3	2.6	2.1	2.1	2.3	2.6	2.3
G	3	Surface	3.3	3.1	3.5	3.8	3.0	2.6	3.0	3.1	3.2	2.6	3.0	2.8
		Middepth	3.1	1.9	3.1	3.6	2.4	2.1	2.6	3.4	2.8	2.4	2.6	2.9
		Bottom	1.9	2.8	2.1	2.3	1.8	3.1	1.8	2.1	2.0	3.3	1.8	1.8
G	Average	Surface	3.9	2.5	4.1	3.9	3.4	2.5	3.6	3.5	3.0	2.0	3.2	3.6
		Middepth	3.4	2.3	3.7	3.5	2.8	2.3	3.1	3.4	2.5	2.0	3.1	3.6
		Bottom	2.6	2.4	3.0	2.3	1.9	2.4	2.4	2.3	2.0	2.2	2.4	2.3

* u.s., undistorted-scale structure; d.s., distorted-scale structure.

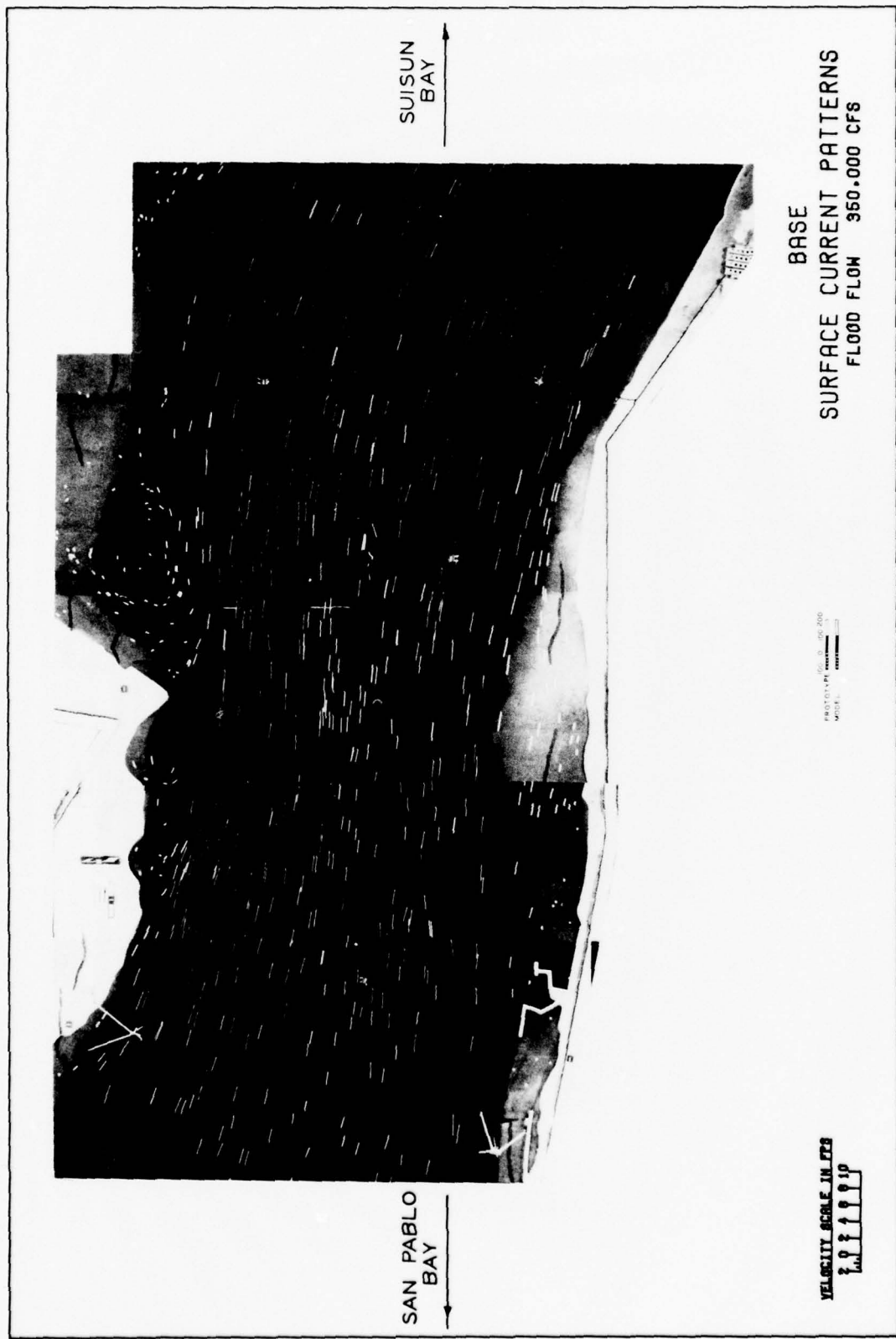


PHOTO 1

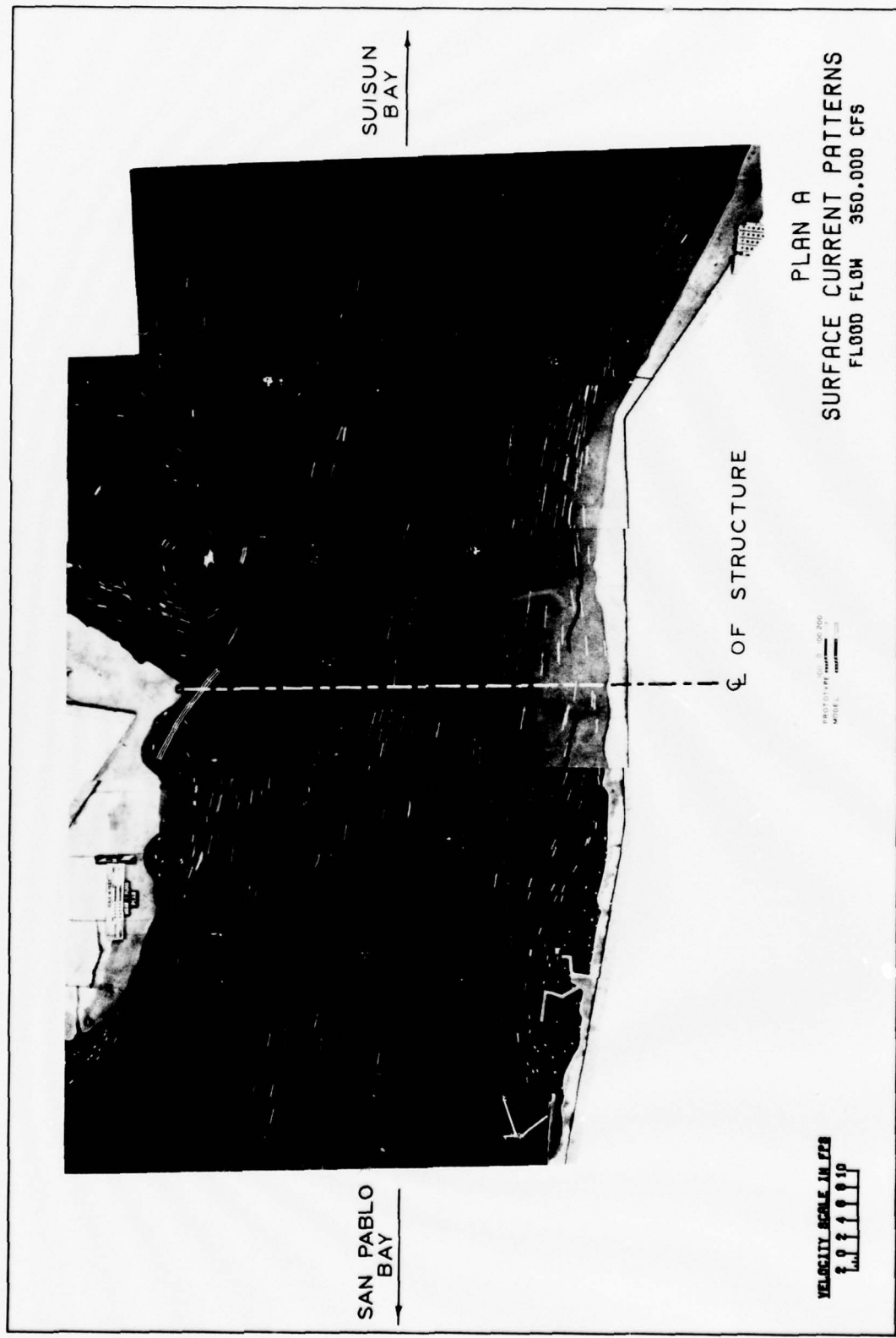
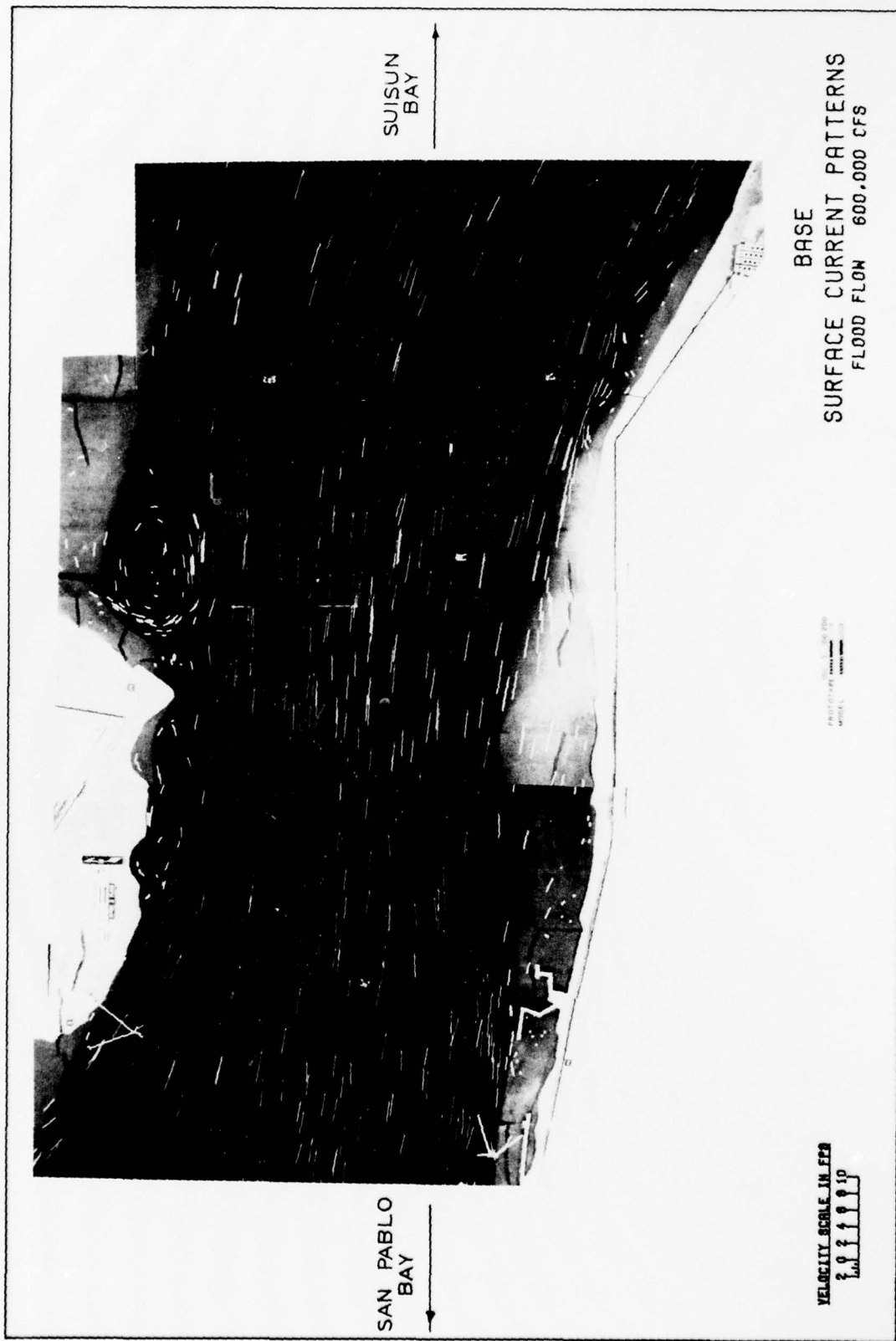


PHOTO 2



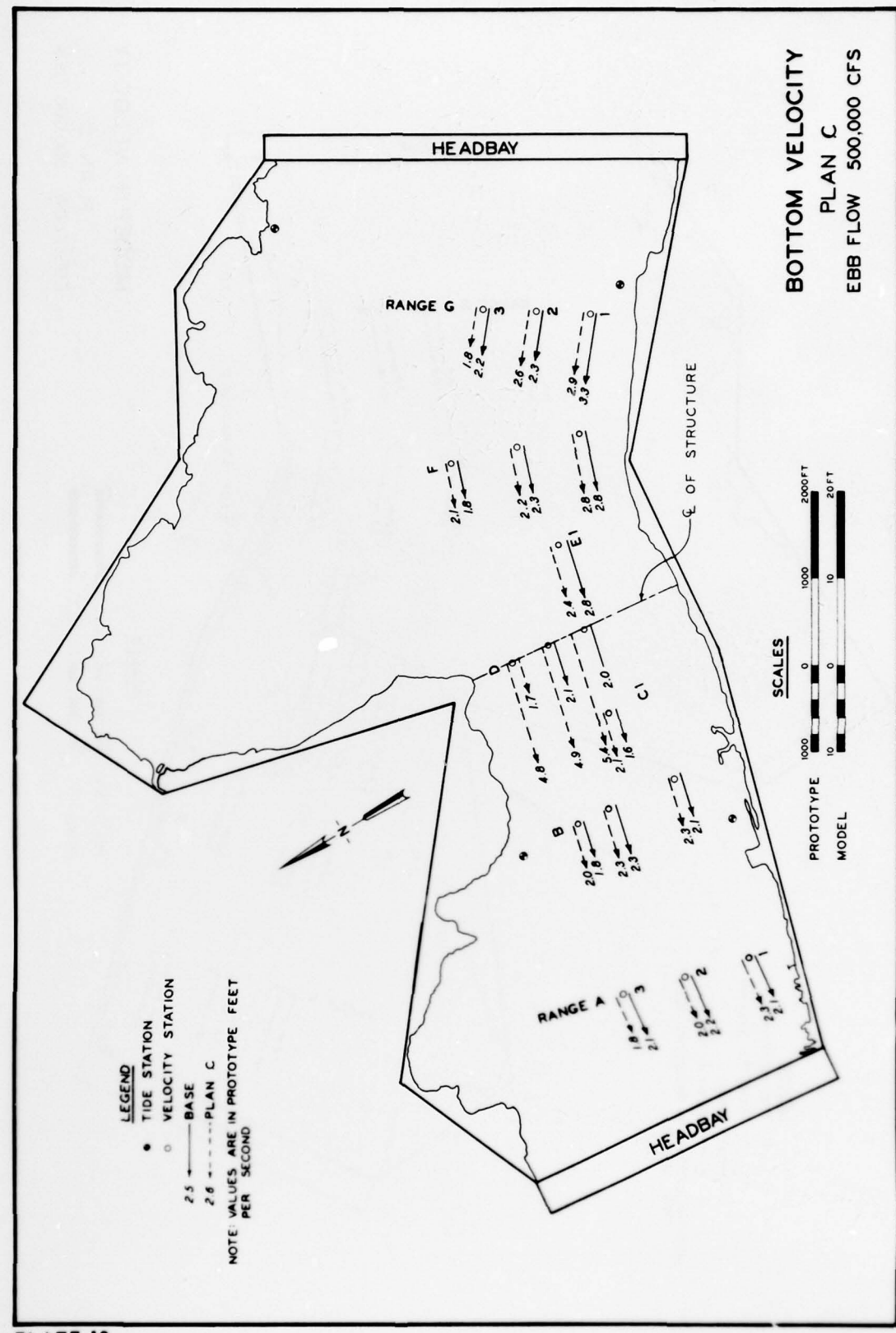


PLATE 18

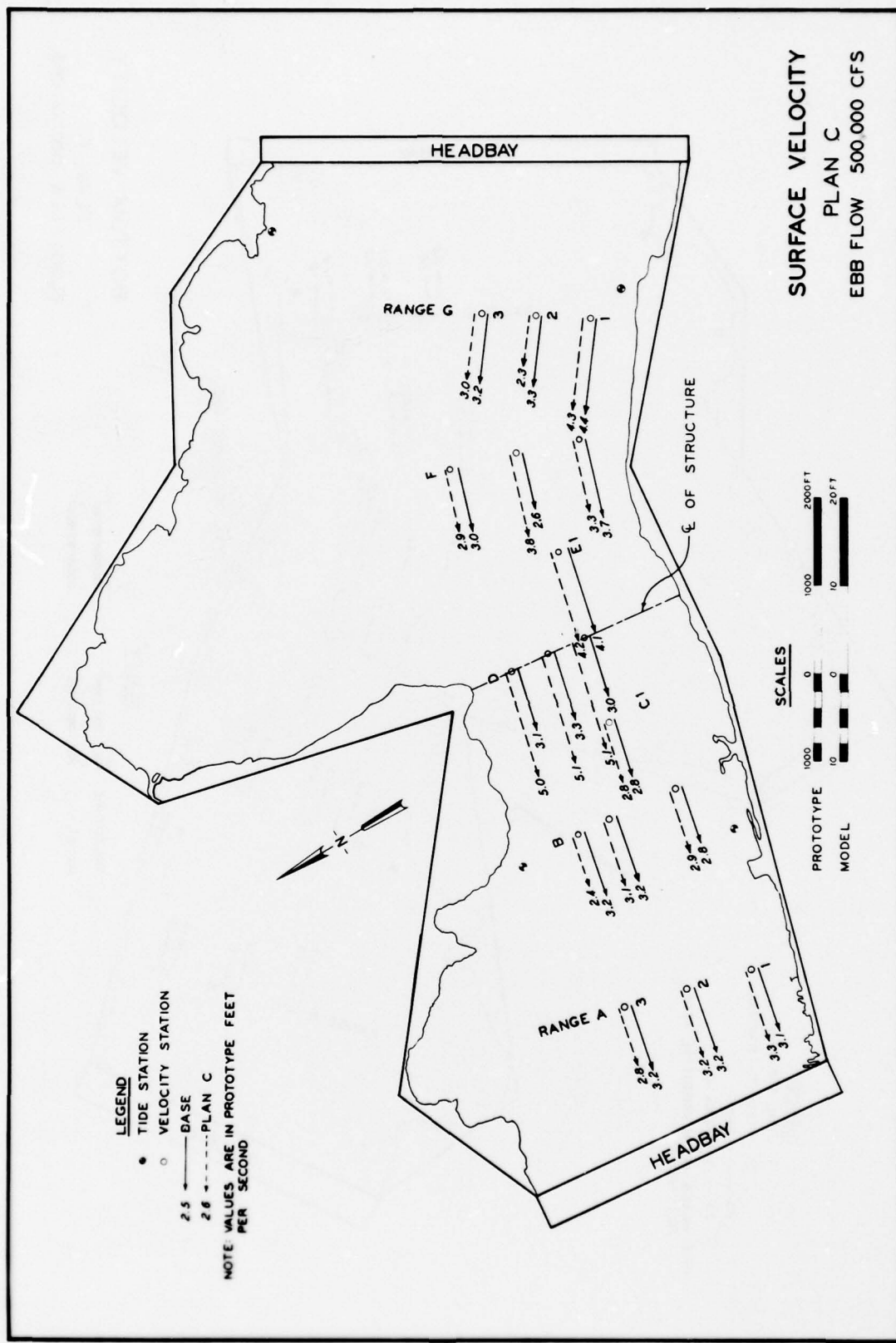


PLATE 16

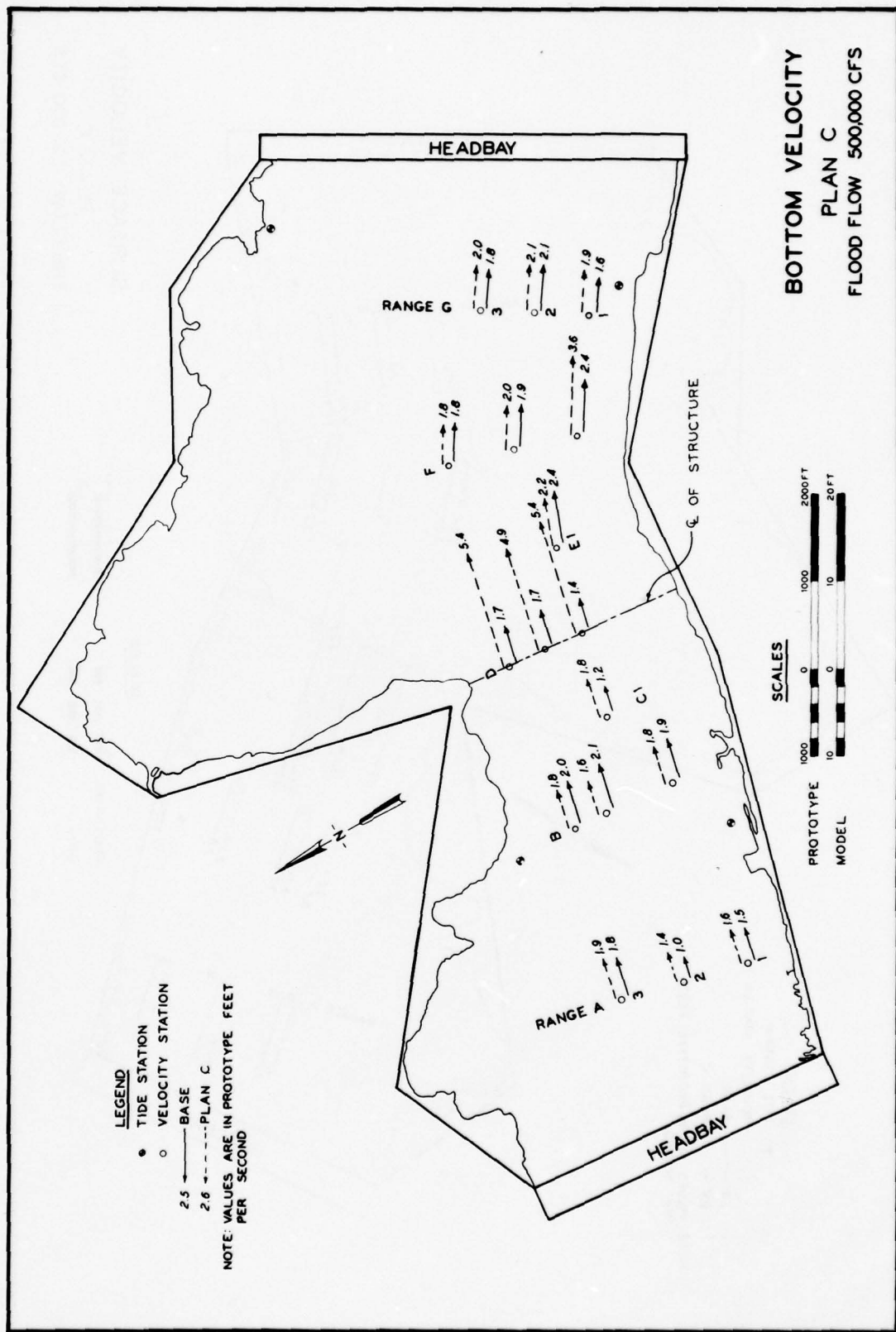


PLATE 15

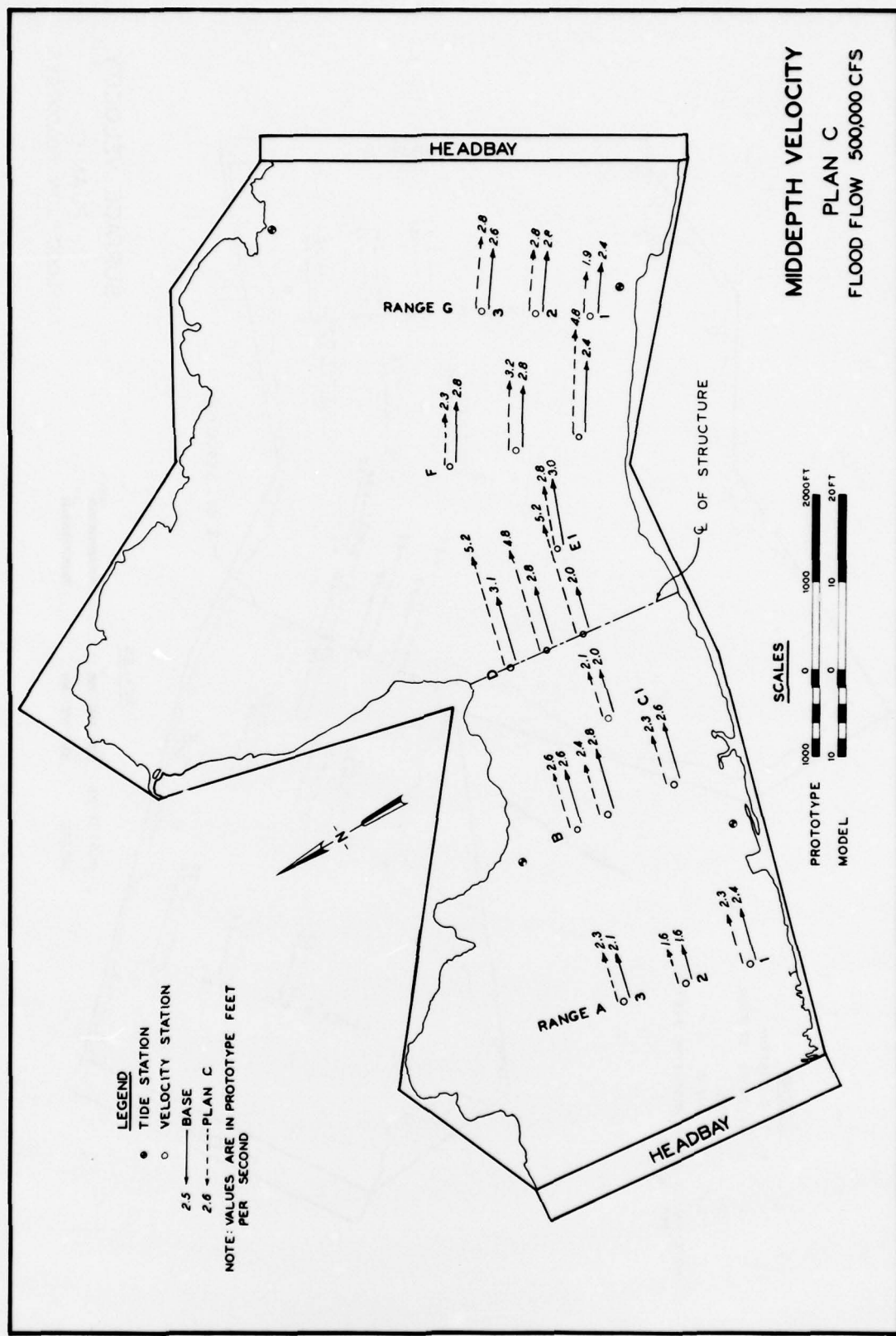


PLATE 14

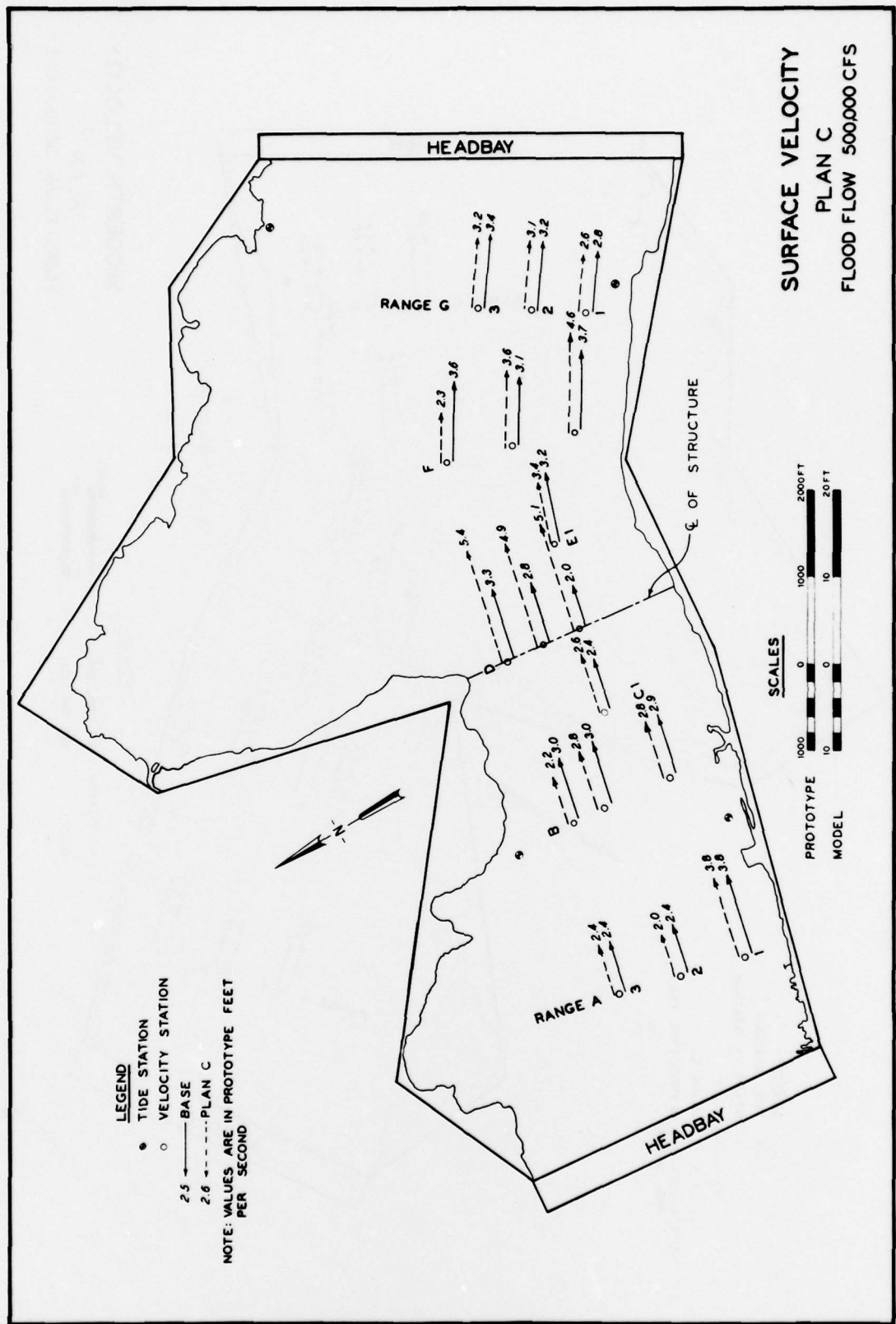


PLATE 13

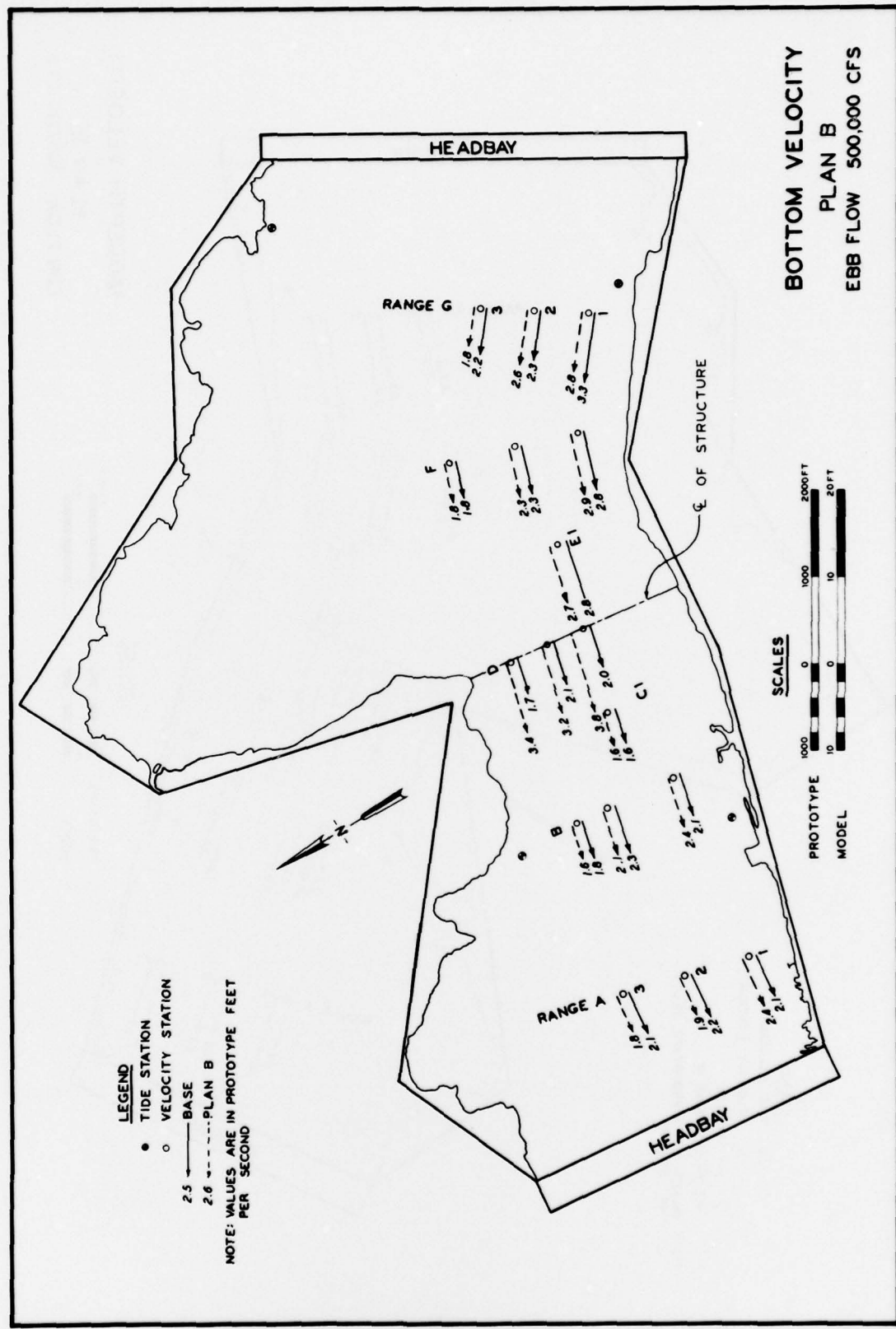


PLATE 12

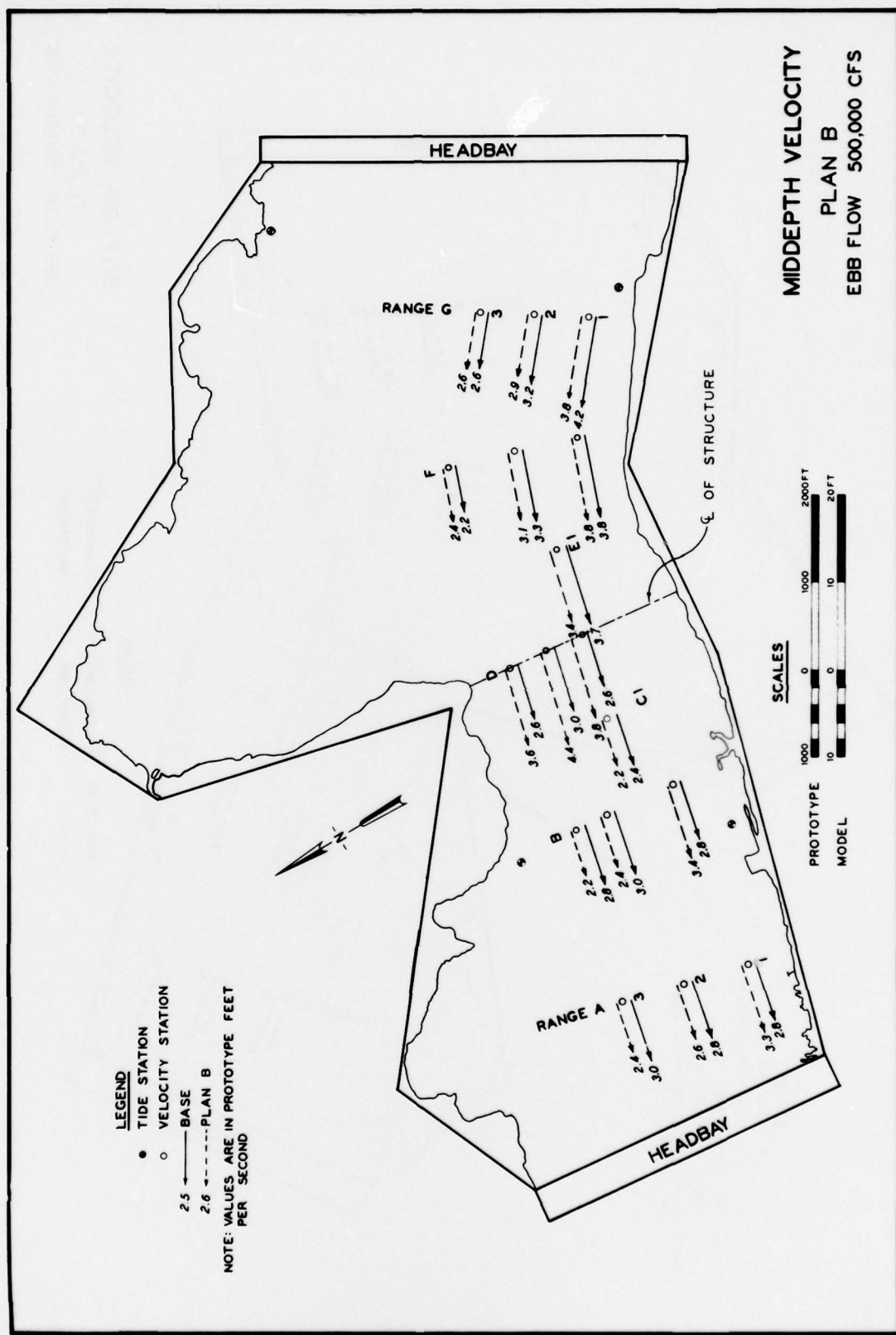


PLATE 11

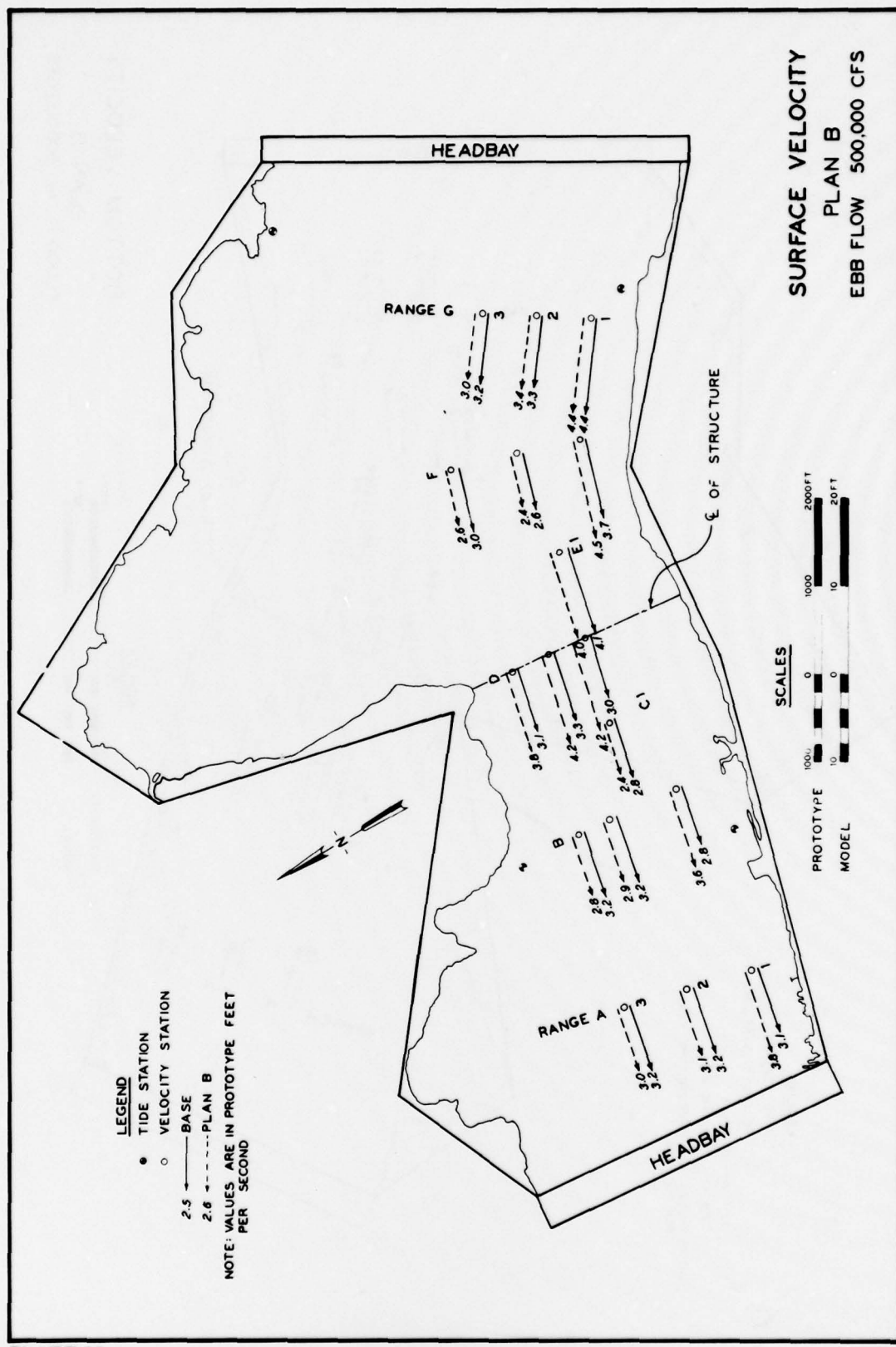


PLATE 10

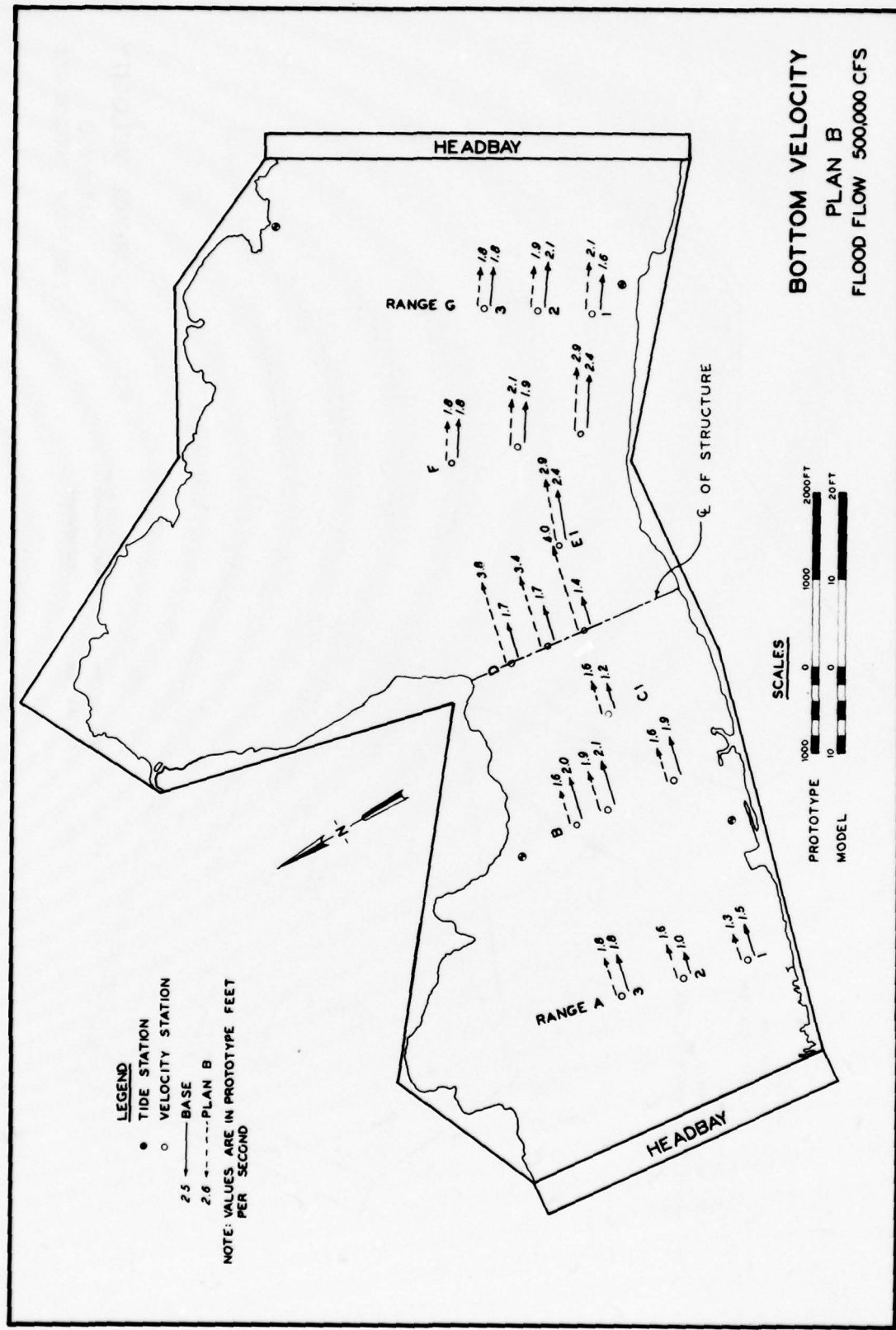


PLATE 9

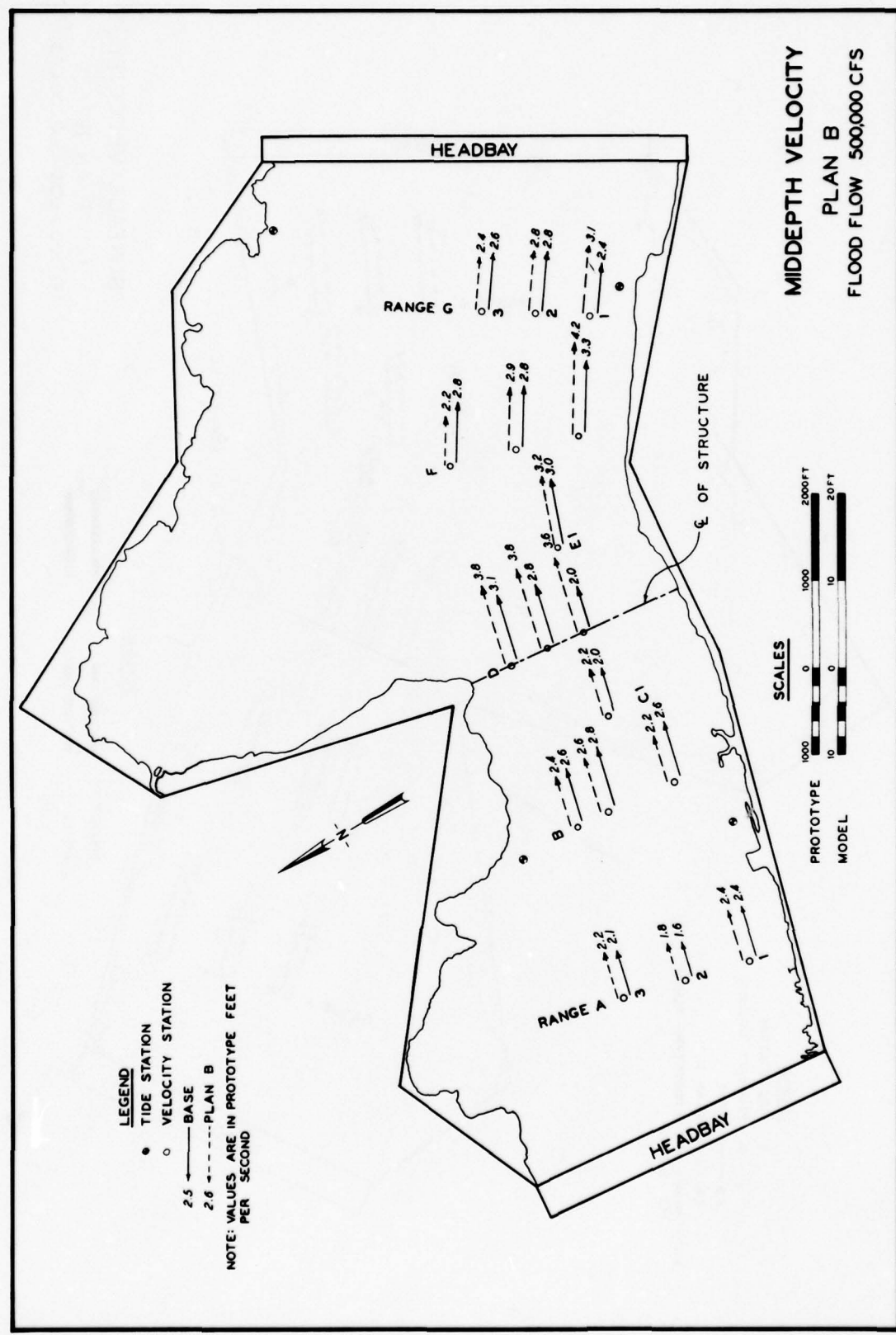
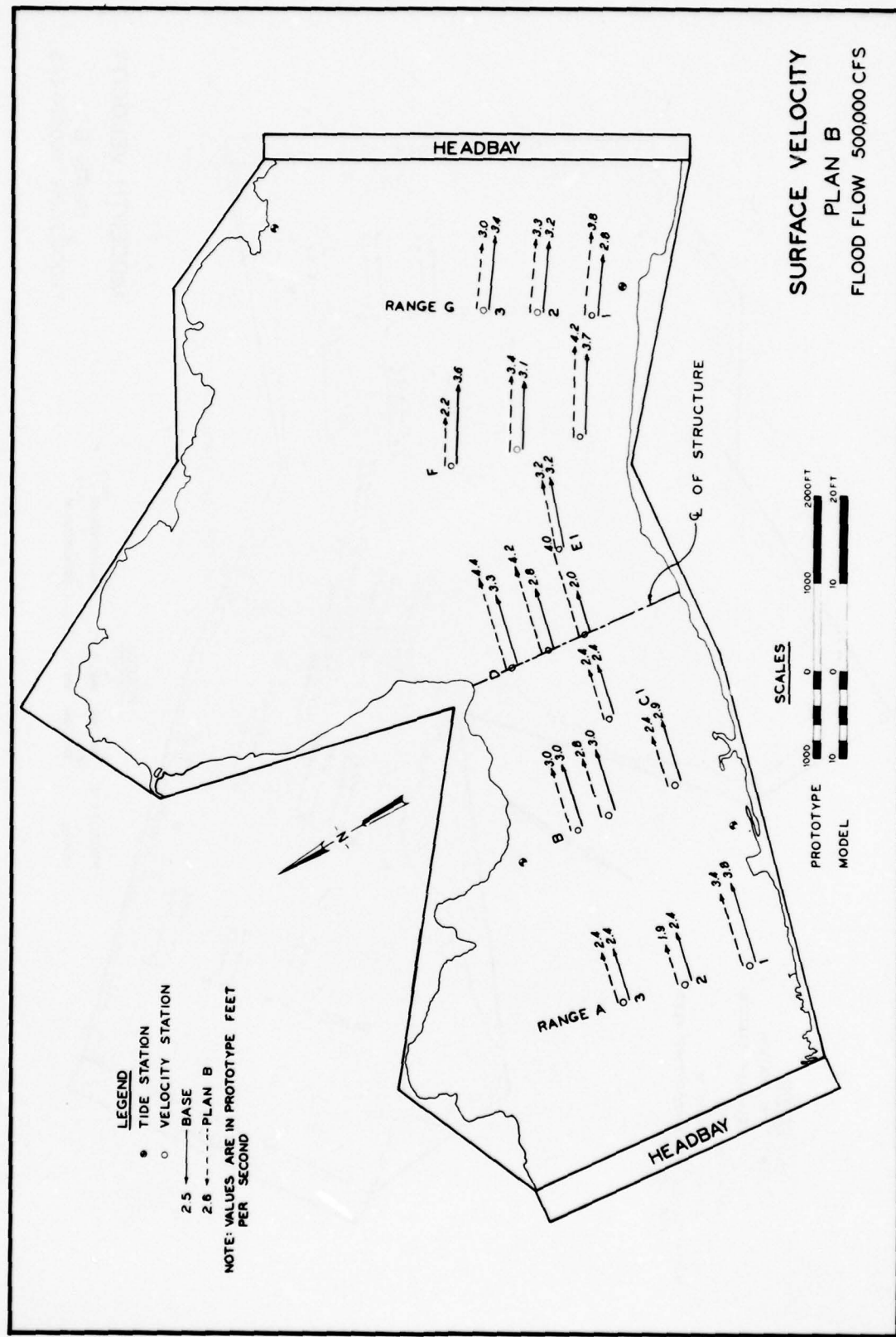


PLATE 8



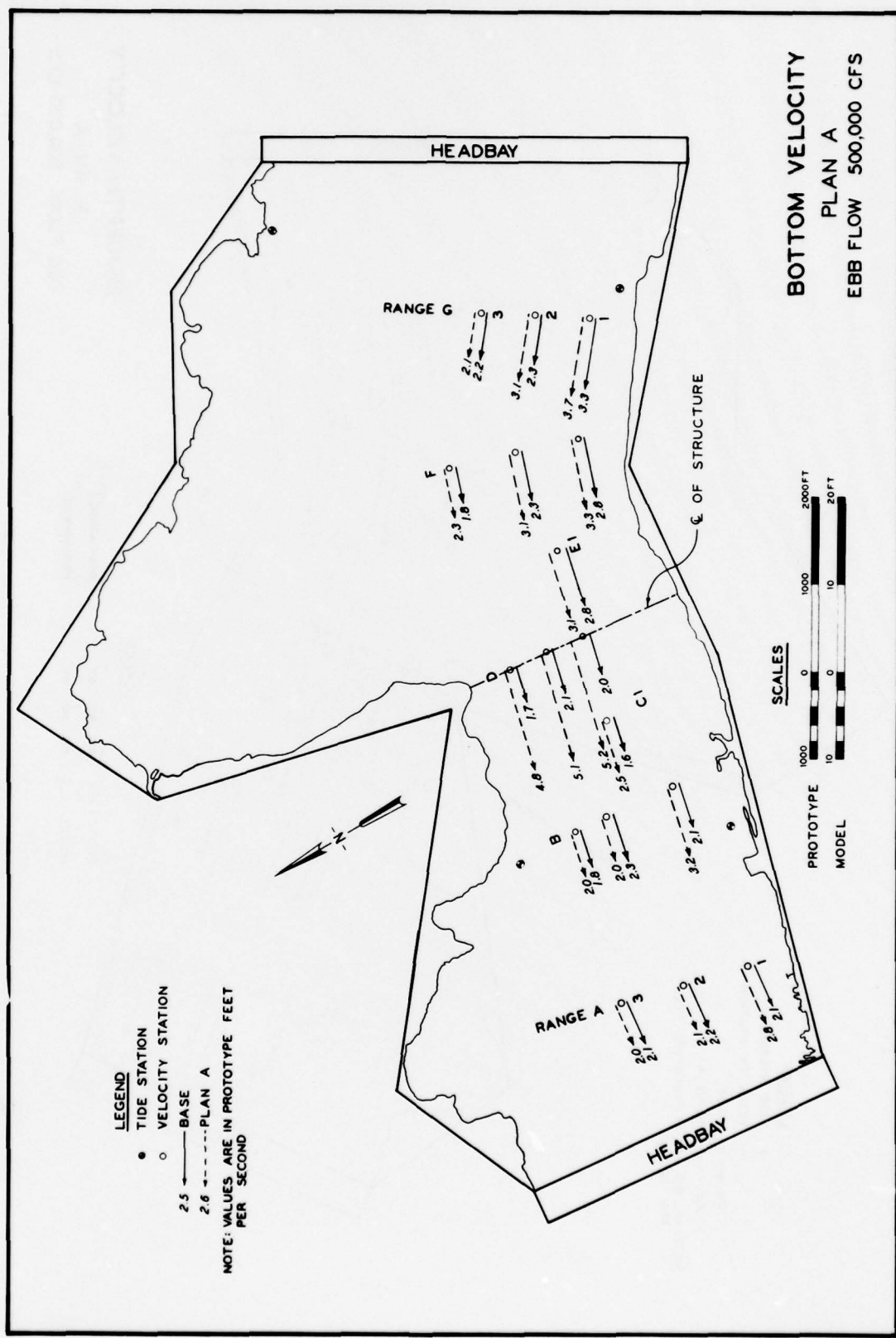


PLATE 6

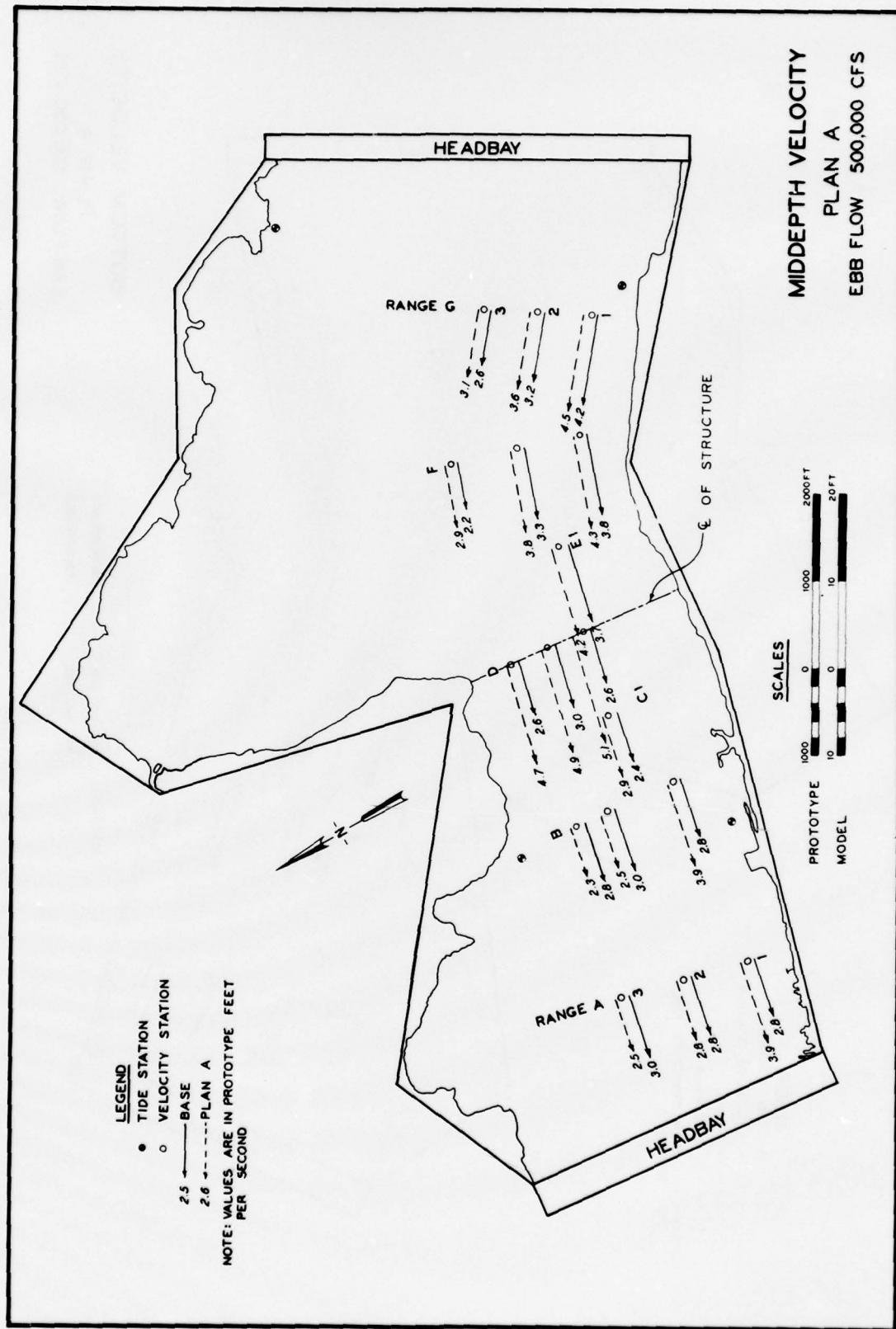


PLATE 5

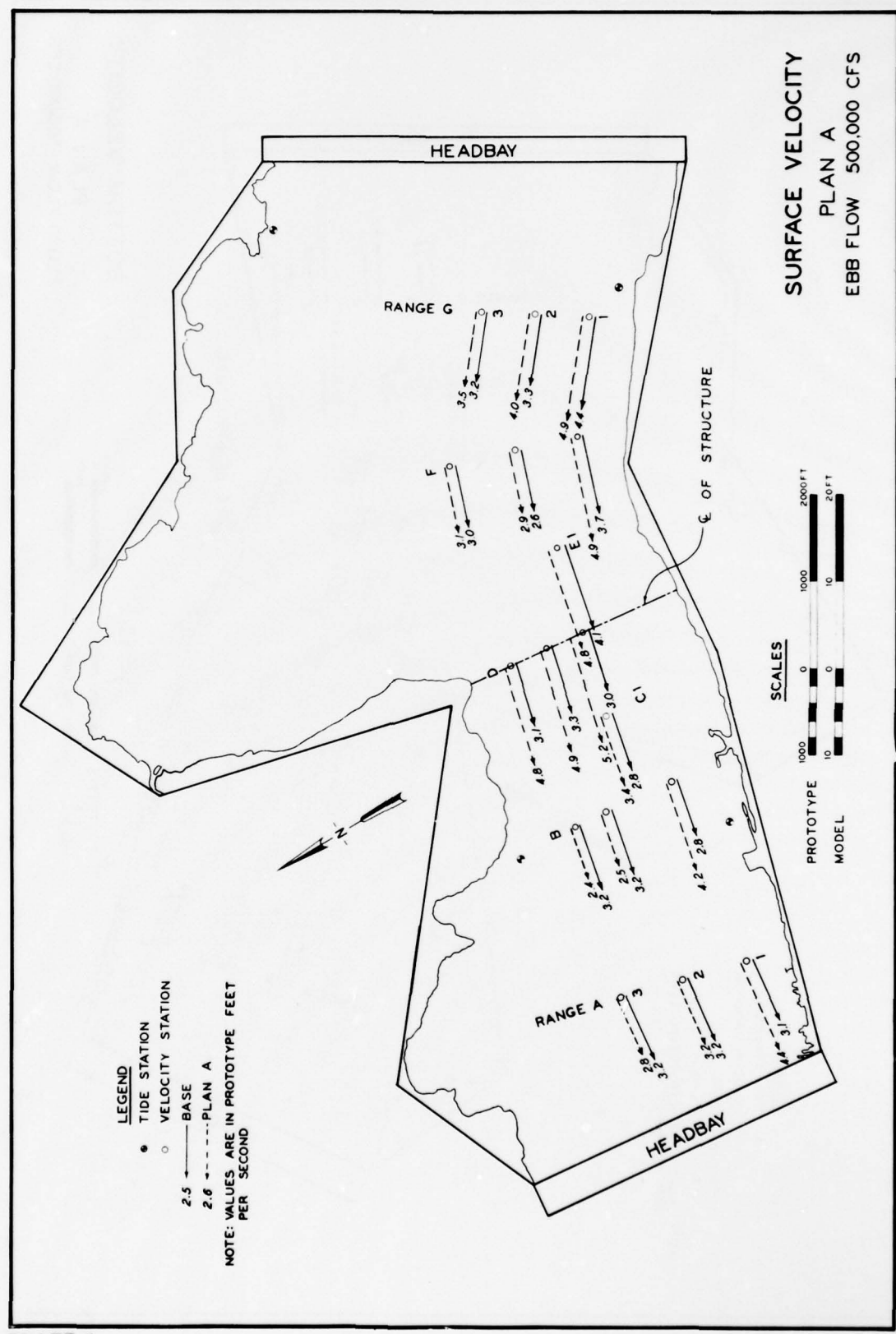


PLATE 4

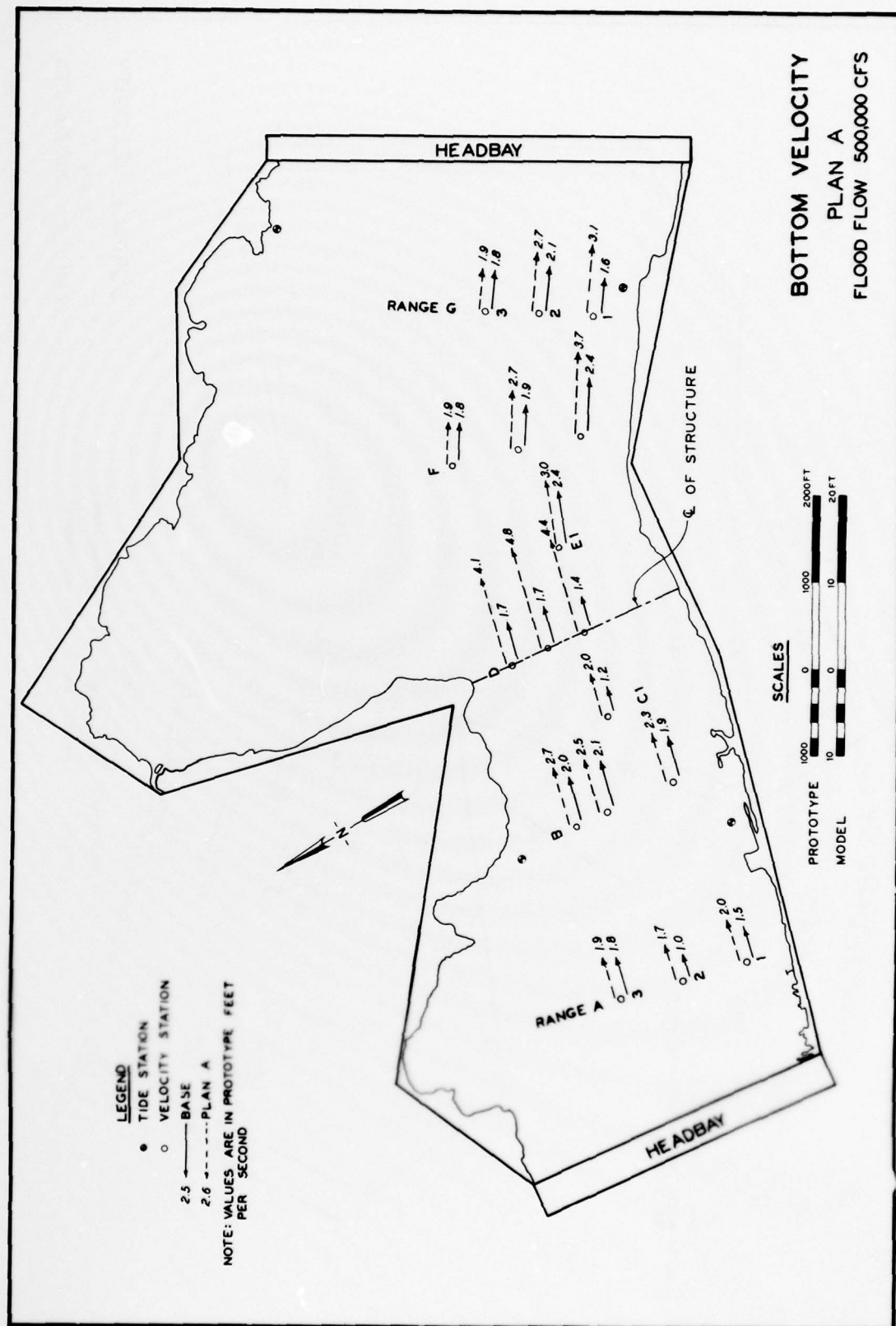
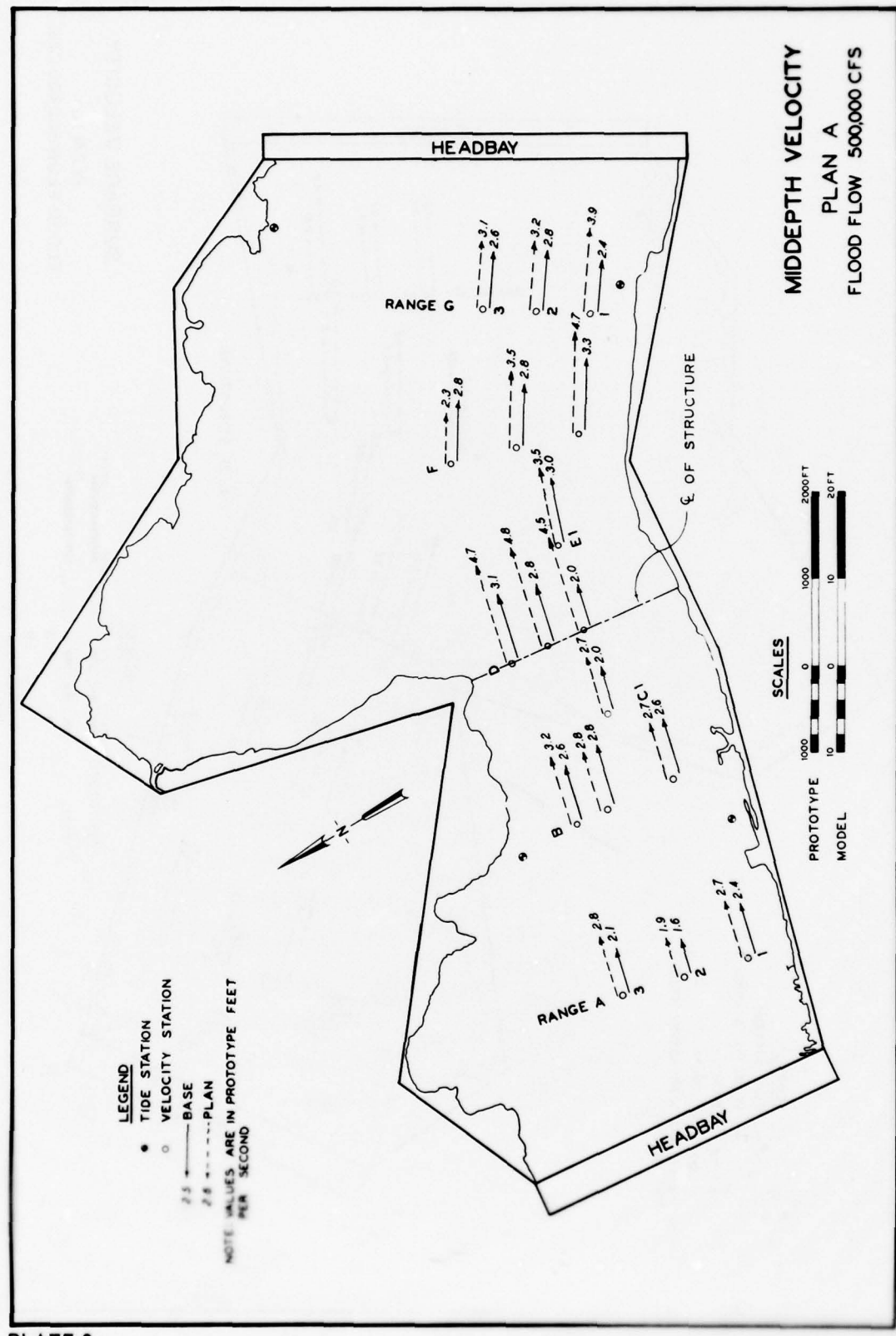


PLATE 3



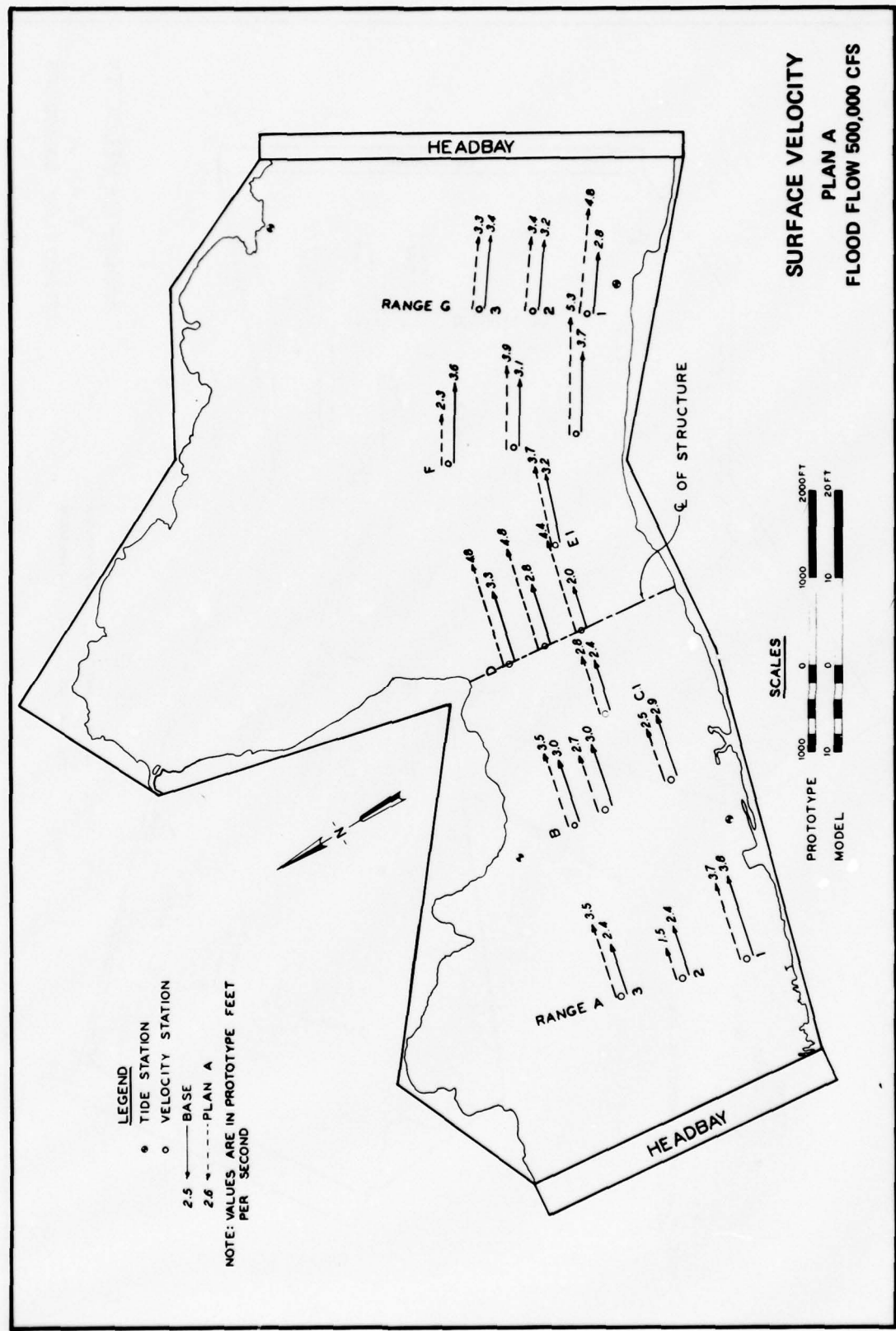


PLATE 1



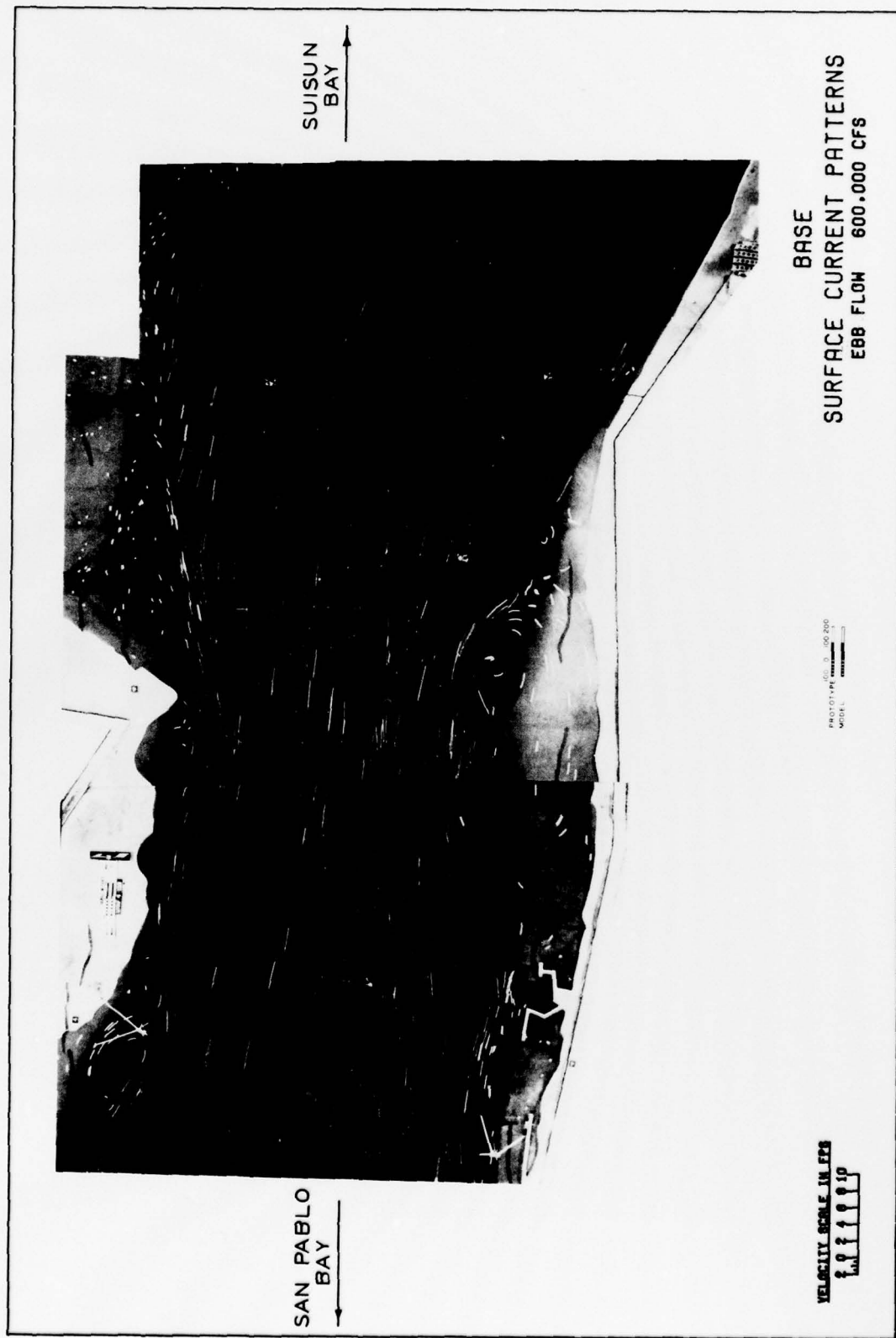


PHOTO 7

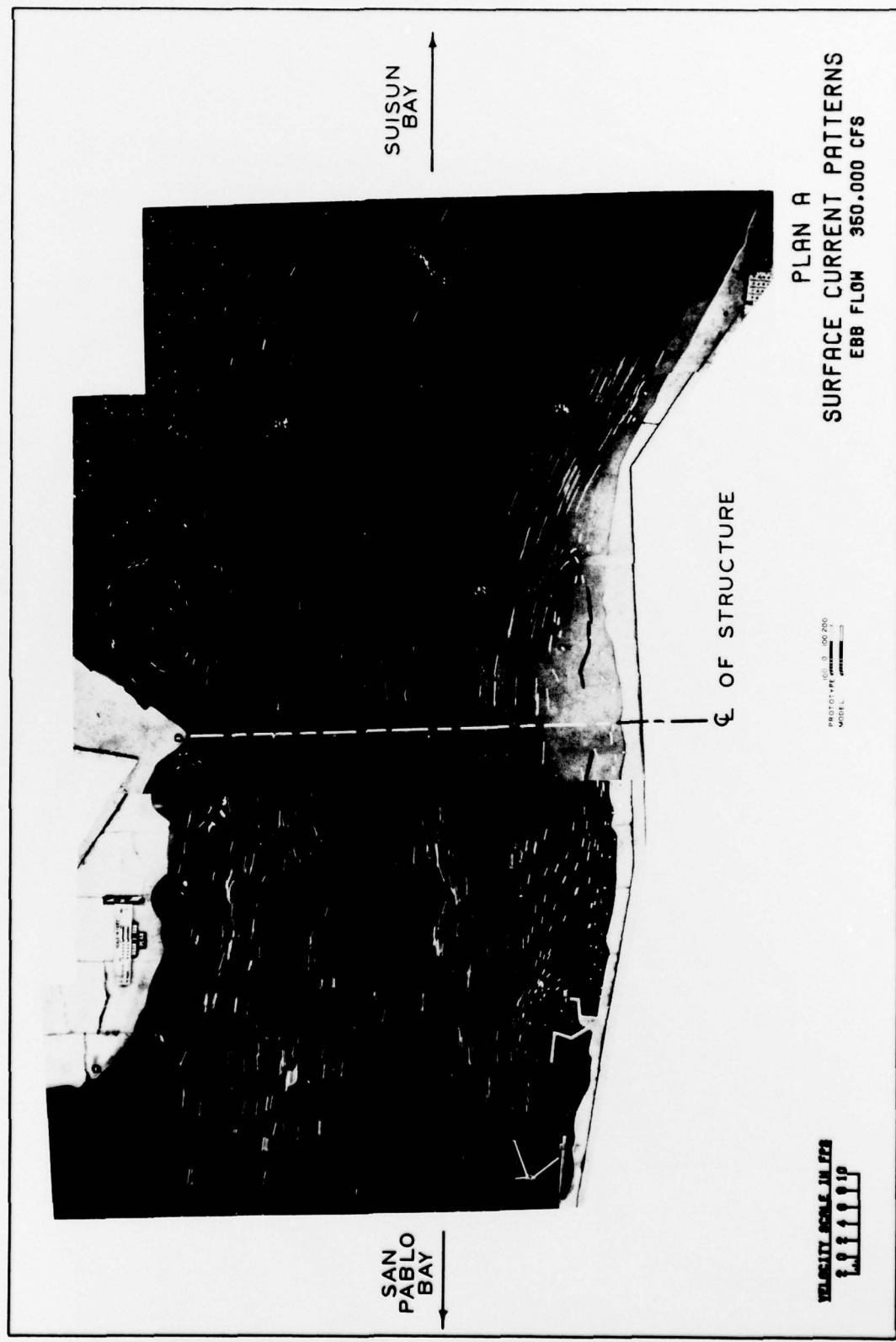


PHOTO 6

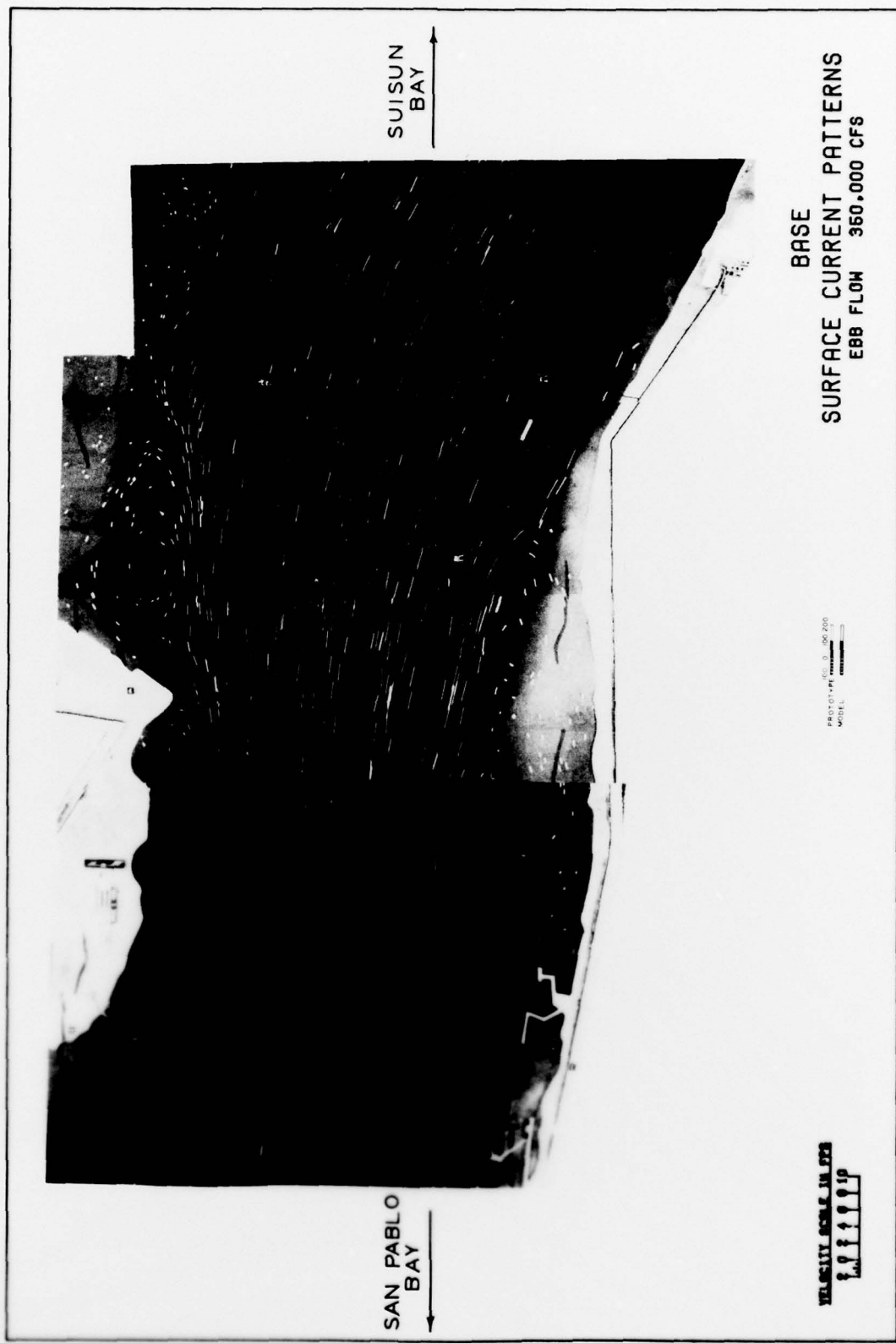


PHOTO 5

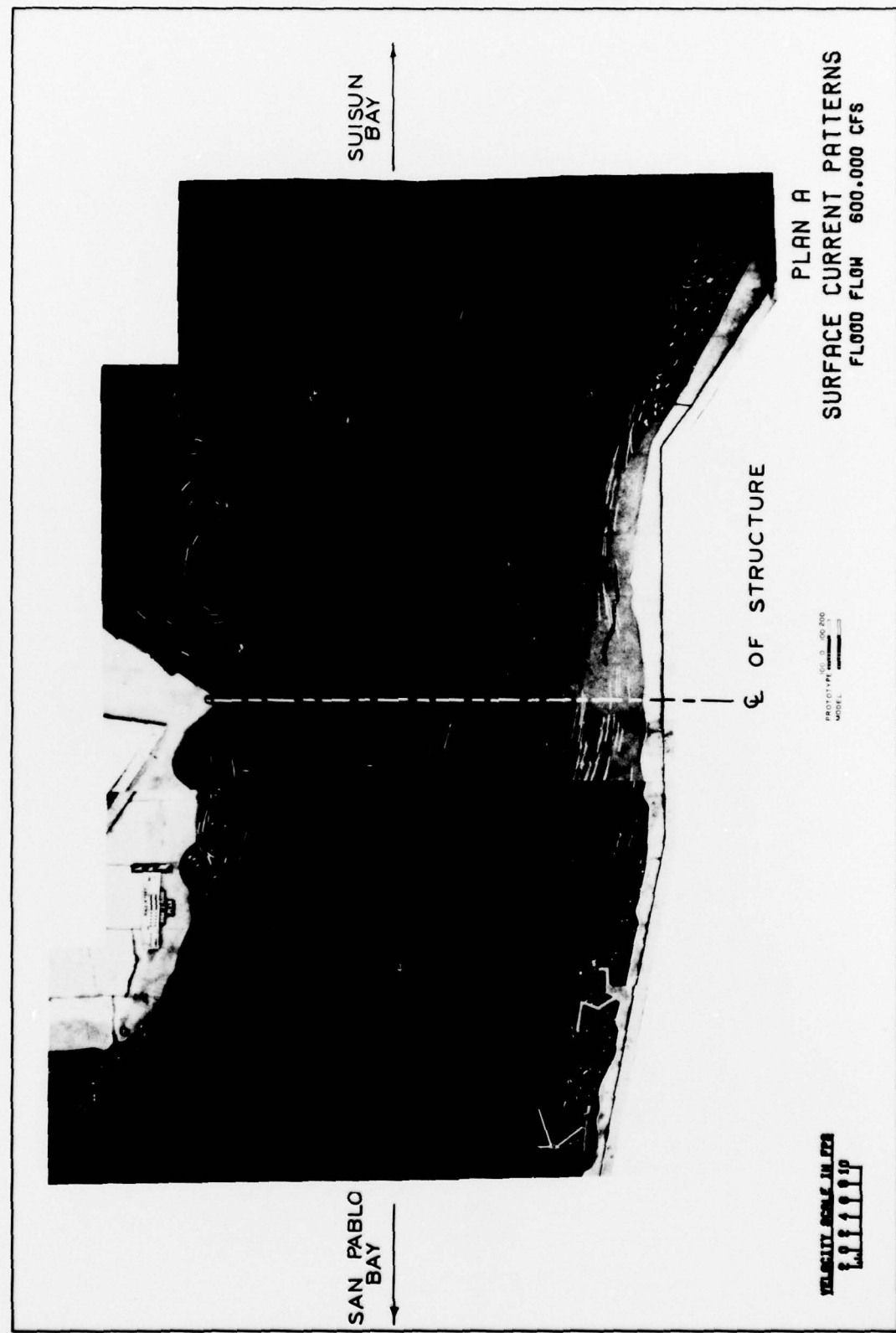


PHOTO 4

APPENDIX A: UNDISTORTED-SCALE PHYSICAL MODEL VERIFICATION

1. Because of the small water-surface differentials and the rapid tidal fluctuations exhibited in the Carquinez Strait, a direct comparison of prototype discharge characteristics in the tidal mode to the 100-to-1 (prototype to model) undistorted-scale physical model discharge characteristics in the steady-state mode was not possible. Therefore, an indirect approach using a numerical model that could be operated in both the tidal and steady-state modes was used to assist in the verification of the undistorted-scale physical model.

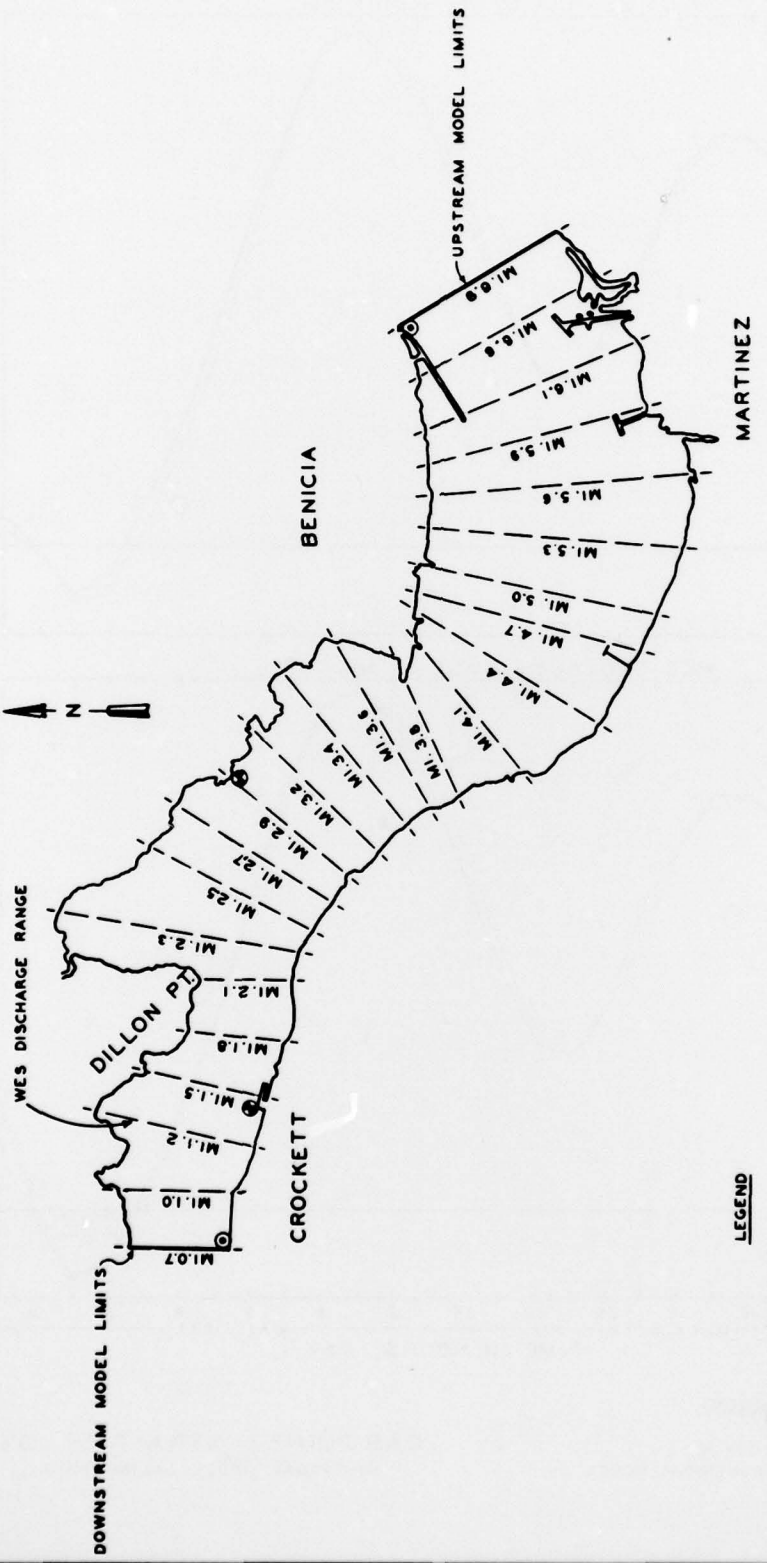
2. The numerical model selected was the one-dimensional HEC "Gradually Varied Unsteady Flow Profiles" model. Documentation of the model may be found in Hydrologic Engineering Center Report 723-G2-L7450, "Gradually Varied Unsteady Flow Profiles," June 1976. The upstream and downstream numerical model limits (dictated by the location of NOAA tide gages for boundary input information), the location of the bottom-elevation cross sections for coding the model, the locations of the WES tide gages, and the discharge measurement range used in the calibration of the model are shown on the location map in Plate A1.

3. The procedure followed was to drive the numerical model at the upstream and downstream boundaries with the NOAA water-surface elevation data collected on 6 and 7 May 1977 at miles 0.7 and 6.9 and compare the model behavior with the observed prototype data collected at miles 1.2, 1.4, and 2.9 by WES on 6 and 7 May 1977. The coefficient for model roughness was adjusted until satisfactory agreement between model and prototype was achieved. This calibration effort resulted in comparisons with the observed prototype tides and discharges as indicated in Plates A2 and A3. Results were considered to indicate satisfactory agreement between numerical model and prototype, and the numerical model was considered to be adequately calibrated.

4. The numerical model was then operated in a steady-state mode for comparison with the undistorted-scale physical model. If the calibrated numerical model was significantly more or less efficient in transporting water than the undistorted-scale physical model (as

determined by the discharge-head relation), the physical model roughness would have to be adjusted accordingly until agreement with the numerical model was achieved. The resulting comparisons of the numerical model with the undistorted-scale physical model with roughness as built in both the ebb and flood directions are shown in Plate A4. Since the agreement between the undistorted-scale physical model and the numerical model was satisfactory, no adjustment of the undistorted-scale physical model roughness was necessary, and the physical model was considered verified for its intended use.

HEC NUMERICAL MODEL LOCATION MAP



M11.0 — LOCATIONS OF CROSS SECTIONS FOR
NUMERICAL MODEL CONSTRUCTION

PLATE A1

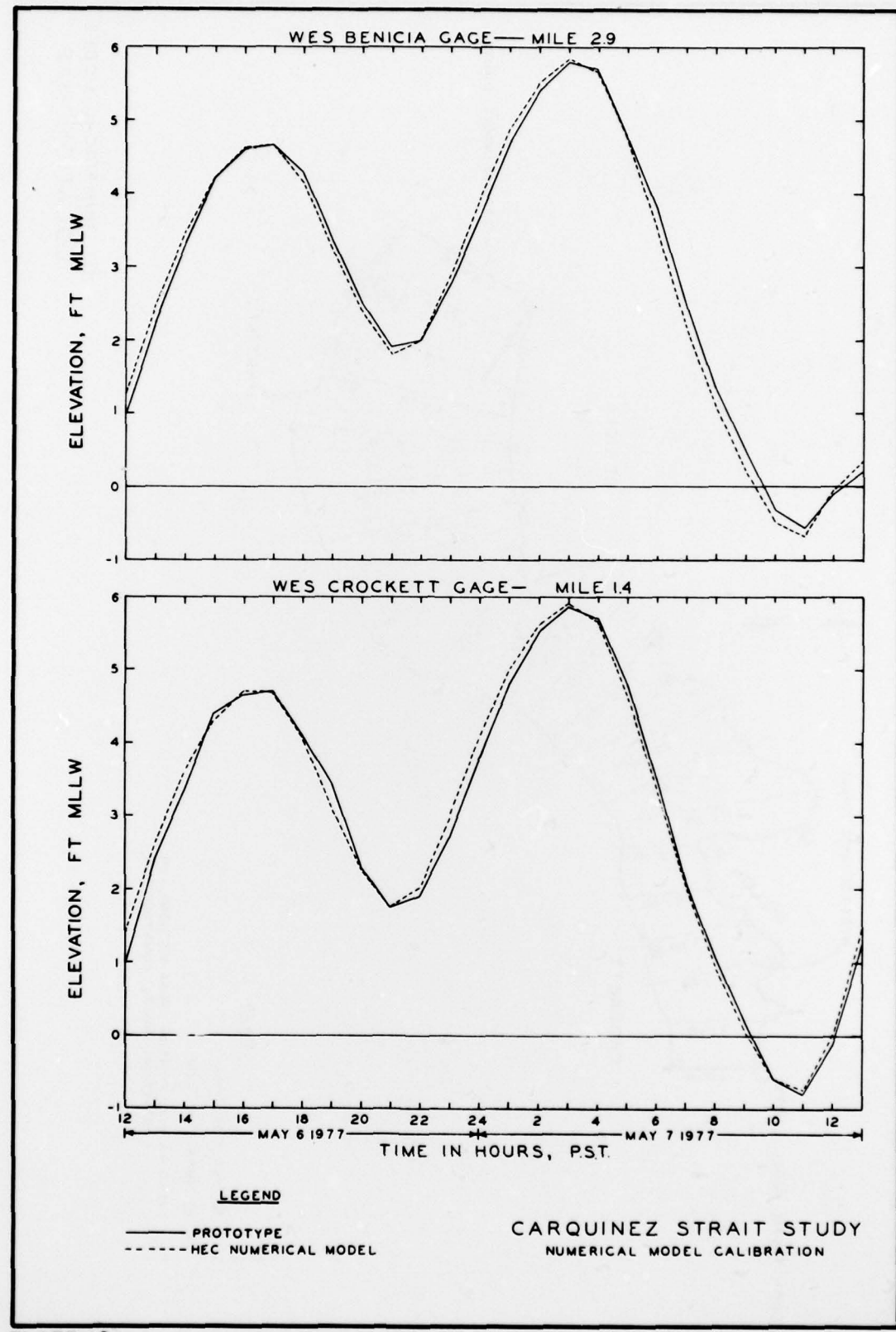
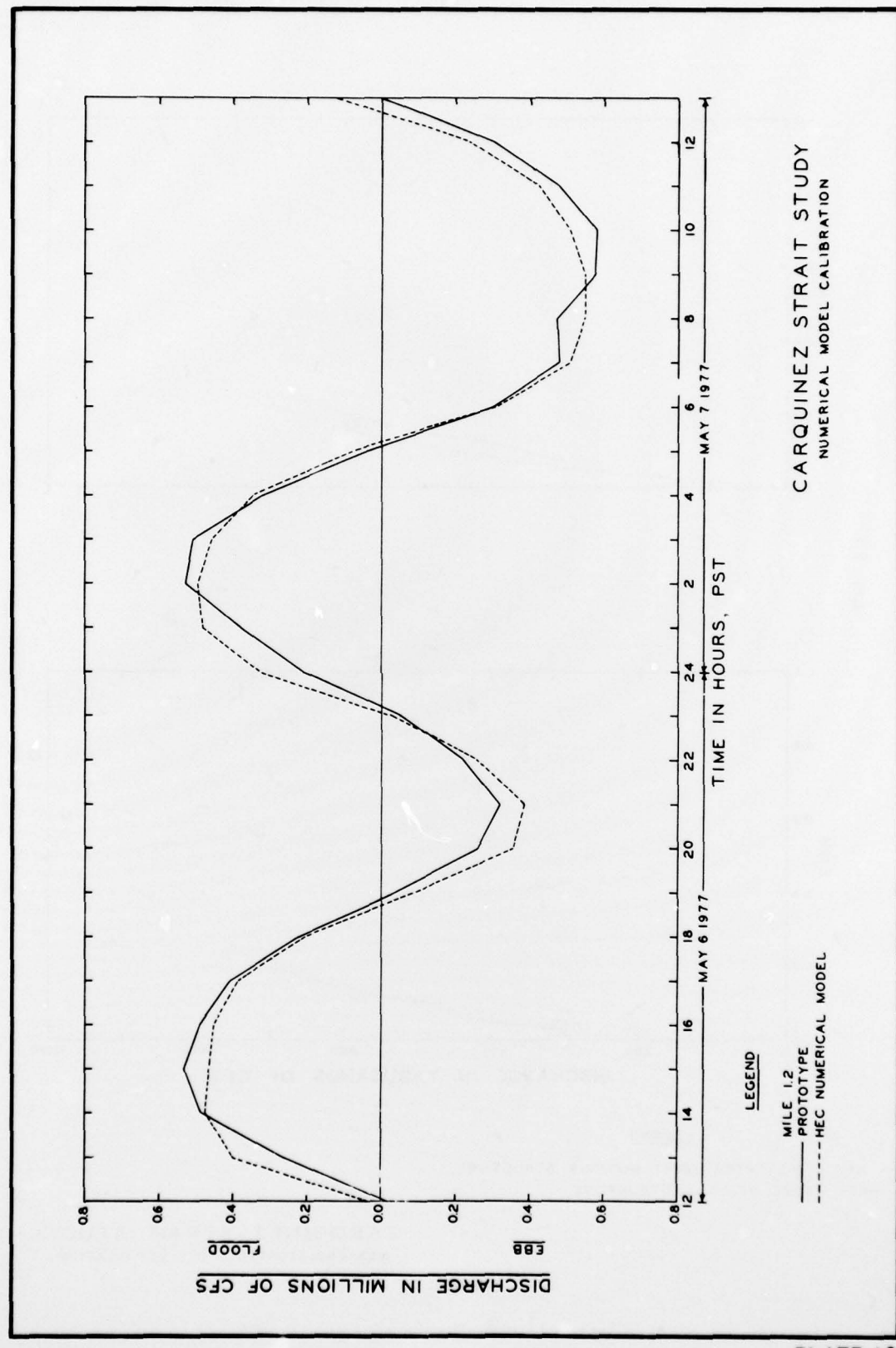


PLATE A2



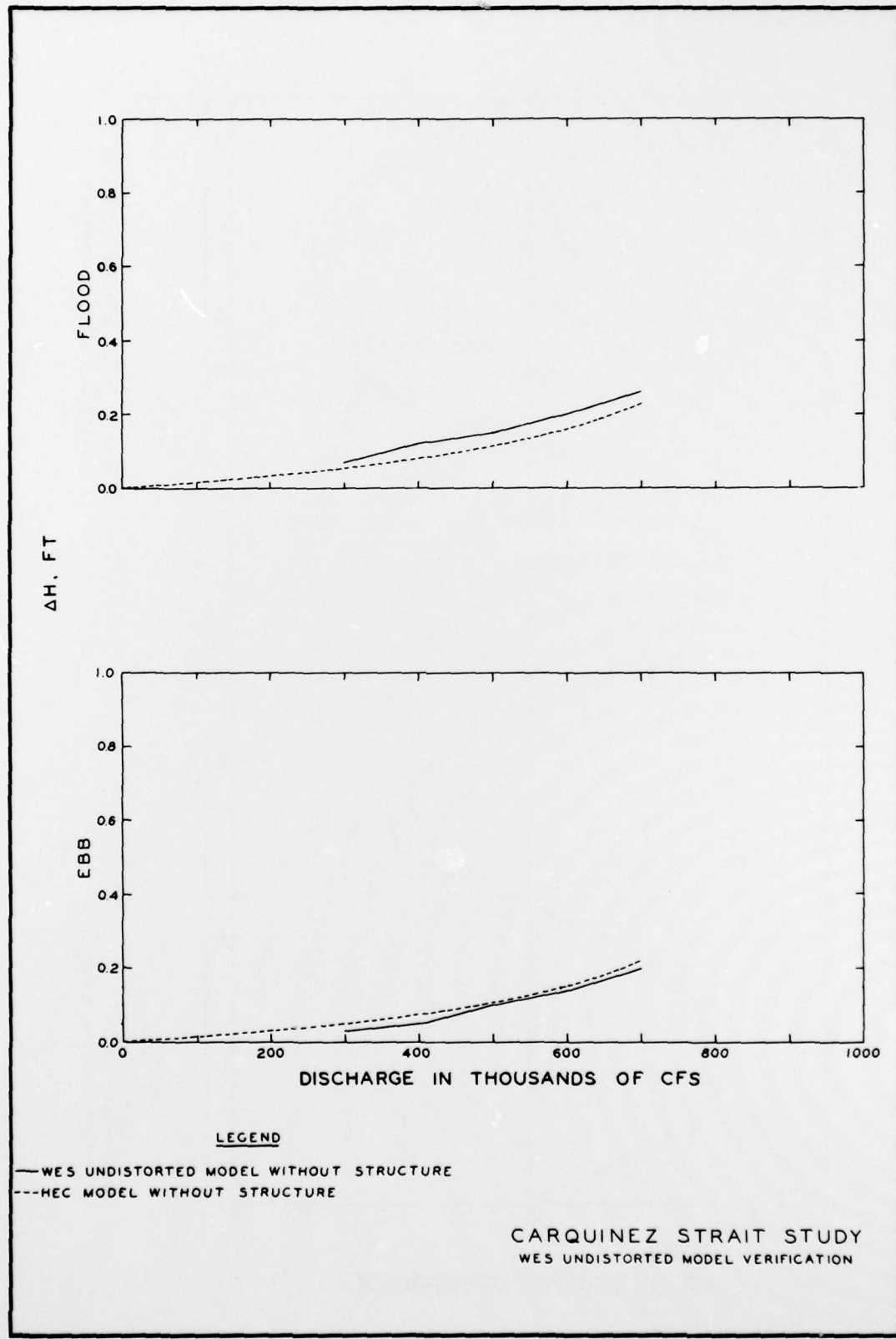


PLATE A4

APPENDIX B: REDUCTION IN DISCHARGE CAUSED BY SUBMERGED SILL:
STEADY-STATE COMPARED WITH TIDAL MODE

1. The undistorted-scale physical section model can provide information concerning the reduction in discharge for a given head differential for the steady-state mode of operation only. One approach to predict the reduction in tidal discharge that would occur in nature as a result of the submerged sill would be to install the sill in the comprehensive San Francisco Bay-Delta model and measure any resulting change in tidal discharge. Another approach to the problem, presented in this appendix, involves the combined use of the undistorted-scale physical section model, the San Francisco Bay-Delta model, and the numerical model described in Appendix A of this report. Preliminary results from the San Francisco Bay-Delta model indicated: (a) tidal elevations at the downstream boundary of the numerical model were not significantly affected by the submerged sill, and (b) the tidal elevations at the upstream boundary of the numerical model appeared to have been slightly reduced in range (reduction of 0.2 ft). Therefore when the numerical model was operated with the submerged sill, the upstream boundary tidal range was reduced by 0.2 ft compared with the existing (no sill) condition, and the downstream tidal elevations were unchanged from the existing condition.

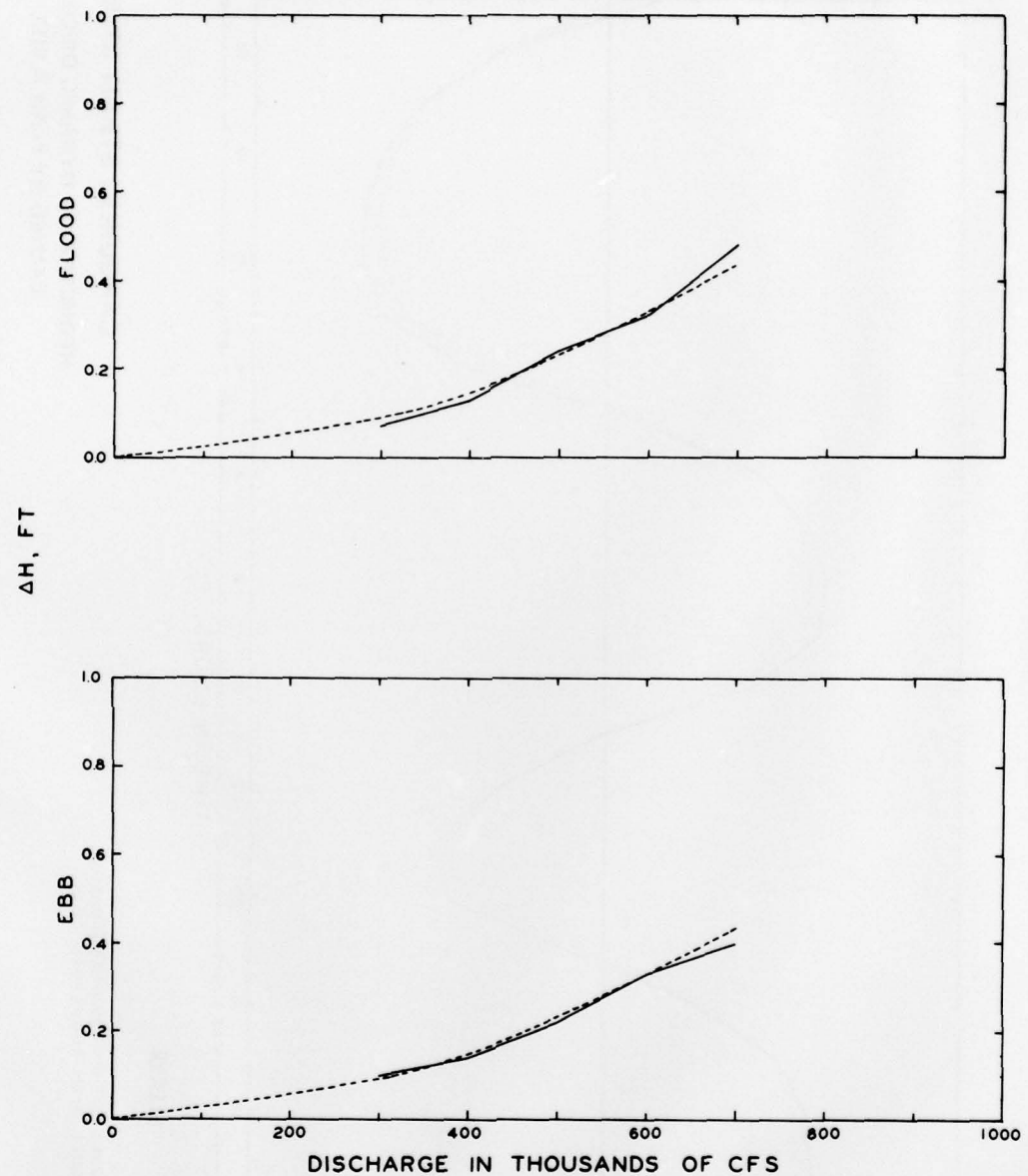
2. The procedure used was to first alter the numerical model described in Appendix A to include the plan A submerged sill (crest el -50). The submerged sill numerical model was then operated in a steady-state mode and the resulting discharge-head relation was compared with the discharge-head relation obtained from the undistorted-scale physical model. The numerical model sill roughness (n value) was adjusted until satisfactory agreement with the undistorted-scale physical model was achieved, at which time the submerged sill numerical model was considered calibrated. The resulting comparison of numerical and physical section models in the steady-state mode is shown in Plate B1.

3. The next step was to run the calibrated numerical submerged sill model in the tidal mode and compare the resulting tidal discharge

with the tidal discharge obtained from the numerical model for existing conditions, as shown in Plate B2. The comparison indicates that in the tidal mode the submerged sill caused only a slight reduction in the tidal discharge of about 6 percent, certainly less than the reduction in discharge experienced in the steady-state mode of operation. For example in the steady-state mode of operation (ebb and flood directions), the reduction in discharge predicted for various head differentials was as follows:

<u>Head, ft</u>	<u>Discharge without Sill, cfs</u>	<u>Discharge with Sill, cfs</u>	<u>Percent Reduction</u>
0.05	285,000	180,000	37
0.10	470,000	315,000	33
0.15	590,000	400,000	32
0.20	670,000	460,000	31

4. The conclusion from the above exercise is that reductions in steady-state discharge are not necessarily indicative of the percent reduction to be expected in the tidal discharge. In the case of the Carquinez Strait submerged sill, the reduction in tidal discharge was predicted to be only a fraction of the reduction in steady-state discharge.



LEGEND

— WES UNDISTORTED MODEL
 - - - HEC MODEL

CARQUINEZ STRAIT STUDY
HEC NUMERICAL MODEL CALIBRATION
WITH PLAN A SILL

PLATE B1

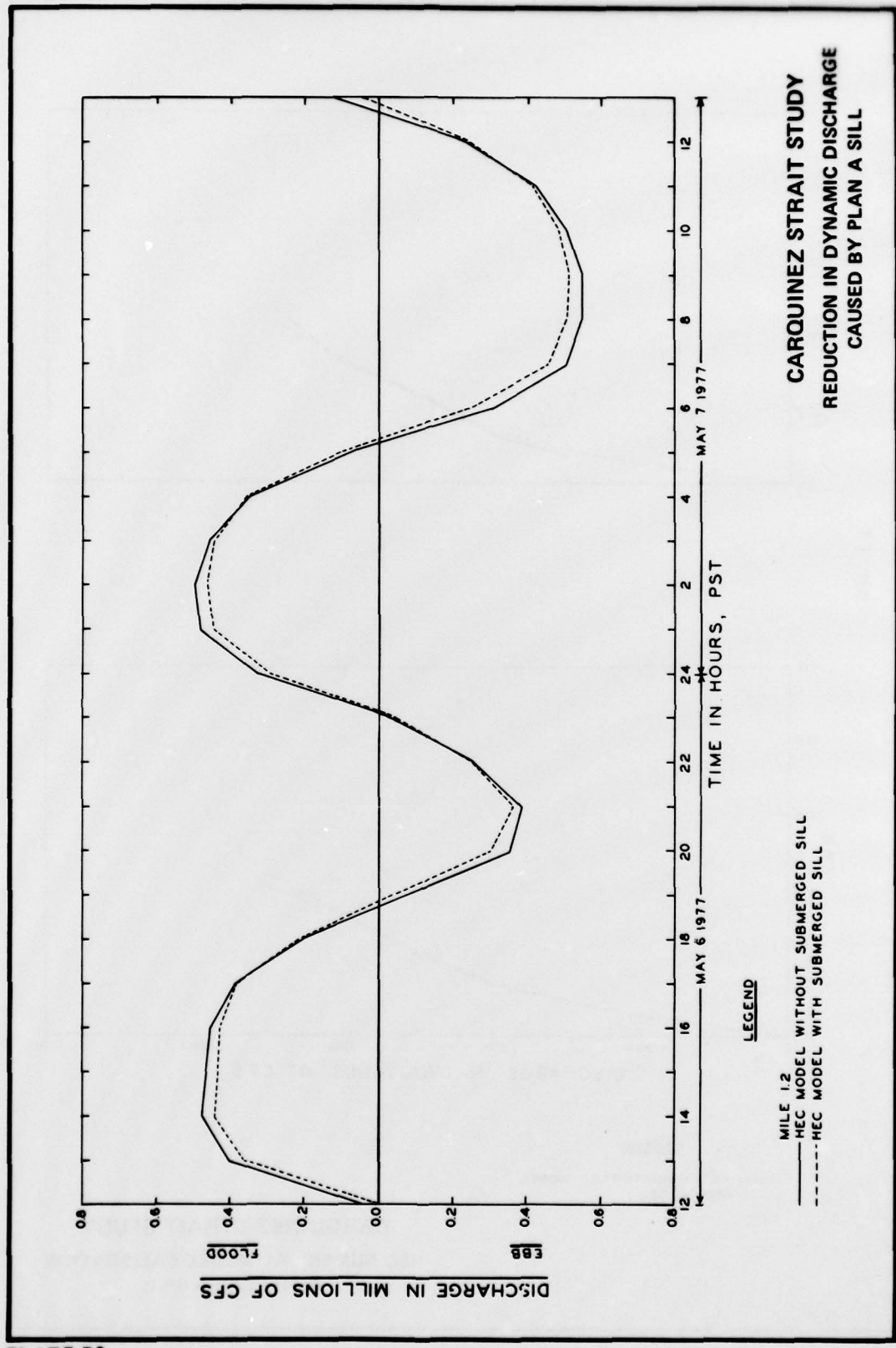


PLATE B2

In accordance with letter from DAEN-RDC, DAEN-ASI dated 22 July 1977, Subject: Facsimile Catalog Cards for Laboratory Technical Publications, a facsimile catalog card in Library of Congress MARC format is reproduced below.

Berger, Rutherford C

Carquinez Strait, California, salinity barrier calibration study; hydraulic model investigation / by Rutherford C. Berger, Jr. Vicksburg, Miss. : U. S. Waterways Experiment Station ; Springfield, Va. : available from National Technical Information Service, 1979.

30, [15] p., [24] leaves of plates : ill. ; 27 cm. (Technical report - U. S. Army Engineer Waterways Experiment Station : HL-79-18)

Prepared for U. S. Army Engineer District, Sacramento, Sacramento, California.

1. Calibrating. 2. Carquinez Strait, Calif. 3. Hydraulic models. 4. Salinity. 5. Salt water barriers. I. United States. Army. Corps of Engineers. Sacramento District. II. Series: United States. Waterways Experiment Station, Vicksburg, Miss. Technical report ; HL-79-18.
TA7.W34 no.HL-79-18.